

UNCLASSIFIED

AD NUMBER

AD870033

LIMITATION CHANGES

TO:

Approved for public release; distribution is unlimited.

FROM:

Distribution authorized to U.S. Gov't. agencies and their contractors; Critical Technology; MAY 1970. Other requests shall be referred to Air Force Avionics Laboratory, AVTL, Wright-Patterson AFB, OH 45433. This document contains export-controlled technical data.

AUTHORITY

afal ltr, 31 may 1974

THIS PAGE IS UNCLASSIFIED

AD870033

(20)
GB

RARE-EARTH DOPED APATITE LASER MATERIALS

Principal Investigators: R.H. Hopkins (phone 412-256-7728)
N.T. Melamed (phone 412-256-3647)
Contributing Authors: T. Henningsen
G.W. Roland

Westinghouse Electric Corporation

Technical Report AFAL-TR-70-103

May 1970



Sponsored by Advanced Research Projects Agency
ARPA Order No. 1467
Program Code No. 9D10/A01467
Contract No. F33615-70-C-1051 *new*
Amount of Contract \$300,000
Contract Dates 9/19/67 to 4/16/71

Air Force Avionics Laboratory
Air Force Systems Command
Wright-Patterson Air Force Base, Ohio 45433



73

| | |
|---------------------------------|--|
| PRINTED FOR | |
| SPECIAL | <input type="checkbox"/> WHITE SECTION |
| LESS | <input checked="" type="checkbox"/> DUFF SECTION |
| UNRESTRICTED | |
| JUSTIFICATION..... | |
| BY..... | |
| DISTRIBUTION/AVAILABILITY CODES | |
| DIST. | AVAIL. and/or SPECIAL |
| 2 | |

NOTICE

When Government drawings, specifications, or other data are used for any purpose other than in connection with a definitely related Government procurement operation, the United States Government thereby incurs no responsibility nor any obligation whatsoever; and the fact that the government may have formulated, furnished, or in any way supplied the said drawings, specifications, or other data, is not to be regarded by implication or otherwise as in any manner licensing the holder or any other person or corporation, or conveying any rights or permission to manufacture, use, or sell any patented invention that may in any way be related thereto.

Copies of this report should not be returned unless return is required by security considerations, contractual obligations, or notice on a specific document.

RARE-EARTH DOPED APATITE LASER MATERIALS

R.H. Hopkins, N.T. Melamed, T. Henningsen, et al

Westinghouse Electric Corporation

Technical Report AFAL-TR-70-103

May 1970

This document is subject to special export controls and each transmittal to foreign governments or foreign nationals may be made only with prior approval of AFAL(AVTL), WPAFB, Ohio.

Air Force Avionics Laboratory
Air Force Systems Command
Wright Patterson Air Force Base, Ohio

FOREWORD

This first semi-annual report covers work performed on the evaluation of rare-earth doped apatite laser materials under Contract F33615-70-C-1051. The work was carried out at the Westinghouse Electric Corporation, Research Laboratories, Pittsburgh, Pennsylvania 15235.

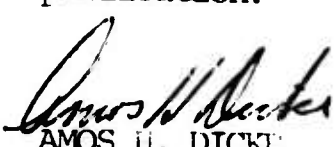
Mr. Richard L. Remski (AVTL), Air Force Avionics Laboratory, Air Force Systems Command, Wright-Patterson Air Force Base, Ohio, is the Project Monitor for this work which is sponsored under ARPA Order Number 1467.

This report was submitted by the authors on 2 April 1970 and covers the period 19 September 1969 to 19 March 1970. Dr. R. Mazelsky, Manager, Inorganic Preparation & Crystal Growth is project supervisor and Drs. R.H. Hopkins and N.T. Melamed are principal investigators. Mr. T. Henningsen has been responsible for laser testing while Dr. G.W. Roland has directed the investigations of crystal chemistry.

We acknowledge the capable assistance of R. Perevuznik and A.M. Stewart in various phases of the experimental work.

APPROVAL:

This semi-annual report has been reviewed and is approved for publication.


AMOS H. DICKIE
Chief, Laser Technology Branch
Electronic Technology Division

ABSTRACT

This first semi-annual report describes the results of the first phase of a program to evaluate the merits of certain members of the mineral family apatite as hosts for the active laser ion holmium.

Of the several silicate oxyapatites (SOAP) studied, preliminary crystal growth and spectroscopic measurements indicated that YSOAP, $\text{CaY}_4(\text{SiO}_4)_3\text{O}$, was the most promising laser host. An initial sensitized host composition, believed near optimum for laser action, was derived from spectroscopic measurements on polycrystalline melt samples. This composition, $\text{CaY}_{2.27}\text{Er}_{1.5}\text{Tm}_{.13}\text{Ho}_{.1}(\text{SiO}_4)_3\text{O}$ forms the starting point for growth of laser quality crystals.

A low temperature, liquid nitrogen-cooled laser testing has been designed and built which is suitable for long pulse, CW, and Q-switched laser operation. The first YSOAP rod grown and tested in this system lased at 77°K with a threshold of 30 joules.

TABLE OF CONTENTS

| | <u>Page</u> |
|---|-------------|
| 1. Report Summary..... | 1 |
| 2. Introduction..... | 3 |
| 2.1 Objectives..... | 3 |
| 2.2 Technical Background..... | 3 |
| 2.3 General Program Approach..... | 5 |
| 3. Current Program Status..... | 7 |
| 3.1 Materials..... | 7 |
| 3.1.1 Experimental Methods..... | 7 |
| 3.1.1.1 Preparation..... | 7 |
| 3.1.1.2 Crystal Growth..... | 9 |
| 3.1.1.3 Methods of Sample Analysis..... | 11 |
| 3.1.2 Material Characterization..... | 12 |
| 3.1.2.1 Melt Samples..... | 12 |
| 3.1.2.2 Single Crystals..... | 13 |
| 3.1.3 Conclusions..... | 21 |
| 3.2 Optimization..... | 23 |
| 3.2.1 Optimization of Rare-Earth Sensitized SOAP. | 23 |
| 3.2.2 Determination of the Best Host..... | 25 |
| 3.2.3 Transfer Considerations..... | 28 |
| 3.2.4 Optimization of Er and Ho in SOAP..... | 31 |
| 3.2.5 Addition of Tm..... | 38 |
| 3.2.6 Other Sensitizers..... | 42 |
| 3.3 Optical Measurements..... | 42 |
| 3.3.1 General Considerations..... | 42 |
| 3.3.2 Fluorescence Emission Measurements..... | 44 |
| 3.3.3 Optical Transmission Spectra..... | 47 |
| 3.3.4 Excitation Spectra..... | 49 |
| 3.3.5 Other Sensitizers..... | 52 |

TABLE OF CONTENTS (cont'd)

| | <u>Page</u> |
|-------------------------------|-------------|
| 3.4 Laser Tests..... | 54 |
| 3.4.1 Apparatus..... | 54 |
| 3.4.2 Laser Measurements..... | 56 |
| 4. Discussion | |
| 4.1 Conclusions..... | 59 |
| 4.2 Future Plans..... | 60 |

LIST OF ILLUSTRATIONS

| | <u>Page</u> |
|--|-------------|
| Fig. 1 Section view of crystal growing furnace (schematic). | 10 |
| Fig. 2 Elongated second phase inclusions commonly found in YSOAP crystals pulled at high rates. Dark areas are shadows of cracks nucleated at the inclusion-matrix interface. Growth direction vertical. Transmitted light, 100X. | 16 |
| Fig. 3 Haloed inclusions observed in heavily sensitized YSOAP crystals. Growth direction vertical. Transmitted light, 500X. | 17 |
| Fig. 4 Globular inclusions developed in YSOAP crystals at slower pull rates. Growth direction vertical. Transmitted light, 200X. | 18 |
| Fig. 5 Precipitate-decorated low angle boundaries in an "a" crystal of sensitized YSOAP. Growth direction normal to plane of paper. Transmitted light, 200X. | 20 |
| Fig. 6 Etch pits delineating low angle boundaries in a chemically polished crystal of LaSOAP. Growth direction undetermined. Reflected light, 200X. | 22 |
| Fig. 7 The dependence of the $5I_7 \rightarrow 5I_8$ fluorescence intensity on Ho^{3+} concentration in SOAP hosts of different compositions. | 26 |
| Fig. 8 Energy levels of some selected trivalent rare-earth ions. | 30 |
| Fig. 9 A schematic of the EXCIFLUOR spectrometer system. The light paths are shown dashed for alternate modes of operation. | 33 |
| Fig. 10 The dependence of the relative brightness of YSOAP upon Er concentration. Curves are shown for three Ho concentrations, with lines drawn only to indicate trends. | 34 |

LIST OF ILLUSTRATIONS (cont'd)

| | <u>Page</u> | |
|----------------|---|----|
| Fig. 11 | Equal brightness contour curves for various concentrations of Er^{3+} and Ho^{3+} in YSOAP. Note two regions of brightness maxima. | 36 |
| Fig. 12 | The dependence of the relative brightness of YSOAP containing 0.1 Ho^{3+} and various concentrations of Tm^{3+} and Er^{3+} . | 39 |
| Fig. 13 | Relative brightness values for YSOAP containing 1.5 Er^{3+} , and various concentrations of Ho and Tm. | 41 |
| Fig. 14 | Room temperature fluorescence of Ho in YSOAP. | 45 |
| Fig. 15 | Fluorescence of Ho in YSOAP at 77°K. (sample 201720-120-2) | 46 |
| Fig. 16 | Optical density of YSOAP single crystals containing 0.1 Ho and different sensitizer combinations as a function of wavelength. Top panel: Ho alone; center panel: Ho+1.0Er; bottom panel: Ho+0.9Er+0.1Tm. The high sloping baseline in the upper panel is due to scattering by ~ 0.5 micron inclusions. Increasing amplitude is increasing absorption. | 48 |
| Fig. 17 | Excitation spectra of three YSOAP samples having compositions similar to those shown in Fig. 16. Top panel 0.1Ho; center panel 0.1Ho+1.0Er; bottom panel 0.1Ho+0.9Er+0.1Tm. Note the distorted shapes of the excitation bands which correspond to different absorption bands. | 51 |
| Fig. 18 | Excitation spectrum of Ho in YSOAP; $\text{Ho}_{0.2}\text{Cr}_{0.1}$. Compare the broad excitation spectrum of Cr with the spectrum of the rare earth sensitizers shown in Fig. 17. | 53 |
| Fig. 19 | Liquid nitrogen cooled laser system. | 55 |
| Fig. 20 | Threshold energy as a function of output resonator reflectivity SOAP 18-203380, 3 mm Dia by 25 mm long, AR coated. | 58 |

1. REPORT SUMMARY

The purpose of this program is to assess the capabilities of certain crystalline materials, members of the apatite mineral family, as hosts for the active laser ion holmium. These materials include fluorapatite (FAP), which has already demonstrated laser action at a two micron wavelength when doped and sensitized with Ho and Cr, respectively, and one member of a promising new series of compounds, silicate oxyapatites (SOAP).

The goal of this initial phase of the program was to select the most promising compound among the various SOAP's and, based upon spectroscopic measurements, to optimize the sensitizer and activator ion concentrations of this material. We have fulfilled both objectives; YSOAP, $\text{CaY}_4(\text{SiO}_4)_3\text{O}$, exhibits bright and efficient fluorescence at two microns and crystals of sufficient quality to show laser oscillation can be grown. In particular, spectroscopic data indicates that the composition $\text{CaY}_{2.27}\text{Er}_{1.5}\text{Tm}_{.13}\text{Ho}_{.1}(\text{SiO}_4)_3\text{O}$ should be near optimum for laser action.

We have designed and constructed a low temperature, liquid nitrogen-cooled laser testing facility suitable for long pulse, CW, and Q-switched laser operation. The virtues of this system are flexibility and convenience: it can handle rods and pump lamps of various sizes and is compatible with existing power supplies, resonator mounts,

detectors and Q-switches.

The first SOAP laser rod grown on this contract was tested in our apparatus at 77°K and lased with a threshold of 30 joules. This rod had a composition $\text{CaY}_{2.9}\text{Er}_{.9}\text{Tm}_{.1}\text{Ho}_{.1}(\text{SiO}_4)_3\text{O}$.

2. INTRODUCTION

2.1 Objectives

The primary purpose of this program is to evaluate the merits of certain crystalline materials belonging to the apatite mineral family as hosts for the active laser ion holmium. These materials are to be assessed relative to other current holmium host materials such as yttrium aluminum garnet (YAG), erbium oxide, and calcium erbium fluoride.

2.2 Technical Background

The hexagonal apatite structure (space group $P\bar{3}m$) is characteristic of a number of compounds, some of which have extremely interesting and useful properties as laser hosts and are currently under intensive investigation at the Westinghouse Research Laboratories. In particular the mineral fluorapatite (FAP), which has the composition $Ca_5(PO_4)_3F$, provided the lowest thresholds and highest efficiency of any currently known Nd laser host.⁽¹⁾ The high efficiency of this host in long pulse operation (slope and overall efficiency of 8% and 6%, respectively, have been obtained) is generally attributed to the favorable site symmetry of the lasing ion in the apatite structure which promotes a broad absorption spectrum.

The unique properties of FAP made it natural as a possible host for Ho as well. Indeed, successful laser action was obtained from Ho activated FAP crystals grown during a program sponsored by the Air

Force Materials Laboratory.⁽²⁾ Laser oscillation occurred at 2.07μ with a threshold of about 20 joules. Successful laser operation is attributed to the addition of Cr which is an effective sensitizer for Ho. The measurements which were made on the first rods grown and tested, represented no attempt to optimize final material composition, crystal growth technique, or the laser system.

Many other varieties of apatite exist in nature or have been synthesized in the laboratory.^(3,4) Of particular interest are those compounds based primarily upon trivalent rare earth cations rather than divalent calcium. One such series of compounds, silicate oxyapatite (which we have named SOAP), has the general chemical formula $MR_4(SiO_4)_3^0$ where M is a divalent ion such as Ca or Sr, and R is a trivalent rare earth, e.g., La, Y or Gd. The relationship of this composition to fluorapatite can be envisioned as replacing 80% of the Ca by rare earth, replacing P by Si and maintaining charge balance by coupled substitution of O for F. Since activating and sensitizing ions such as Ho, Er, and Tm can be more readily substituted for the rare earth constituent in SOAP than for Ca in FAP, this new family of apatite materials should provide exceptionally good hosts for laser action.

We have synthesized compounds having the compositions $CaLa_4(SiO_4)_3^0$, $CaY_4(SiO_4)_3^0$ and $CaGd_4(SiO_4)_3^0$ (LaSOAP, YSOAP or GdSOAP, respectively). X-ray analysis of small crystal fragments by the Burger precession method combined with etch pit methods confirmed that these materials do belong to space group $P\bar{6}_3/m$. The SOAP's all melt above $2000^\circ C$ and are much harder and stronger than fluorapatite. The refractive indices of the

SOAP's are near 1.8 compared to 1.63 for FAP and their birefringence, as in all apatites, is low.

Further, we have prepared polycrystalline samples of the various SOAP's containing Ho and various sensitizer combinations of Er and Tm as well as Cr. Preliminary data showed that the Ho fluorescence in SOAP was efficient and bright. One sample of YSOAP had an integrated intensity greater than a laser rod of "ABC" YAG. Small single crystals of La and YSOAP doped with Ho were also grown by the Czochralski method prior to the inception of this program. While these early crystals suffered variously from second phase inclusions and iridium oxide entrapment it was apparent that such difficulties could probably be surmounted by proper control of growth parameters and furnace design so that laser quality crystals could be obtained.

The presence of efficient Ho fluorescence in SOAP, coupled with the ability to grow crystals of these materials make the SOAP's very attractive as new and efficient hosts for two micron laser emission.

2.3 General Program Approach

The properties of FAP:Ho,Cr have been better defined than those of SOAP thus the first objective of the program is to raise our knowledge of the properties of SOAP to the level of FAP. The second goal is then to determine the optimum sensitizer combinations and concentrations for Ho in the SOAP chosen. We will then investigate the areas of interest common to both materials including crystal growth, spectroscopy and active laser testing.

In brief the program consists essentially of four phases:

1. Polycrystalline samples of the various Ho-doped SOAP's will be prepared with and without sensitizers and examined spectroscopically. The properties of FAP:Ho,Cr are known in detail at this level and hence this material is excluded from the preliminary studies. The best SOAP host for holmium will be chosen on the basis of initial spectroscopic measurements, any available pertinent physical or chemical property data, and preliminary crystal growth evaluations.
2. Both FAP:Ho,Cr and the best sensitized SOAF will be optimized with respect to dopant and sensitizer composition on the basis of spectroscopic and laser tests of early crystals grown. Initial crystal growth refinement will begin and physical property measurements will be initiated.
3. Laser crystal growth will be optimized and active laser tests undertaken to determine the capabilities of apatite hosts in pulsed, CW, and Q-switched operation.
4. The laser properties of the optimized apatite hosts will be compared with those of other current holmium hosts.

Progress in the various areas of the program outlined above are discussed in detail in the following sections.

3. CURRENT PROGRAM STATUS

3.1 Materials

3.1.1 Experimental Methods

3.1.1.1 Preparation

In order to survey the many compositions required to choose the "best" SOAP host and then optimize its concentration with respect to fluorescence brightness, we prepared polycrystalline melted samples.

This technique has distinct advantages. Samples can be produced in a rapid and efficient manner. By quenching material from the molten state the normal segregation of doping ions occurring during crystal growth can be almost completely suppressed so that the composition of the solidified sample corresponds to that of the weighed charge. We have previously used this method with success to optimize the Ho and Cr concentration in FAP.⁽²⁾

We followed a strict materials preparation schedule to assure that any sample composition could later be reproduced. Raw materials consisted of Mallinkrodt Standard Luminescent Grade CaCO_3 and silicic acid, American Potash and Chemical Corporation rare earth oxides (stated purities: Y_2O_3 - 99.99, La_2O_3 - 99.997, Er_2O_3 - 99.9, Ho_2O_3 - 99.9, Tm_2O_3 - 99.9, and Gd_2O_3 - 99.9) and Fisher Reagent Grade Cr_2O_3 . Powdered quartz was also used as a source of silica with no apparent effect on spectroscopic properties.

About fifteen grams of each composition were weighed on an analytical balance according to the stoichiometric formula of the host, Y, L or GdSOAP. Doping or sensitizing ions were substituted in desired proportion for the host rare earth cation. The sample powders were rotary mixed for ten minutes, charged into a carefully cleaned iridium crucible, and melted by induction heating in the crystal pulling furnace described in Section 3.1.1.2. We homogenized each melt by maintaining the temperature 20°C above the sample melting point for twenty minutes. The melt was then quenched by shutting off the power. Samples suitable for spectroscopic, microscopic, or X-ray diffraction analysis were then punched from the polycrystalline mass formed during freezing.

We prepared over seventy polycrystalline samples in the above manner. Broadly, the samples fall into the following classes by composition:

1. Singly-doped, $\text{CaR}_{4-x}\text{Ho}_x(\text{SiO}_4)_3\text{O}$, $0.01 < x < 0.4$, where R = La, Y or Gd.
2. Doubly-doped, $\text{CaR}_{4-(x+y)}\text{Er}_y\text{Ho}_x(\text{SiO}_4)_3\text{O}$, $.01 < x < .2$ and $0.5 < y < 4-x$
3. Triply-doped, $\text{CaR}_{4-(x+y+z)}\text{Er}_y\text{Tm}_z\text{Ho}_x(\text{SiO}_4)_3\text{O}$, $0.02 < x < 0.15$, $.05 < z < .15$ and $.75 < y < 3.5$.
4. Miscellaneous, $\text{CaR}_{4-(x+y)}\text{Cr}_y\text{Ho}_x(\text{SiO}_4)_3$, $0.01 < y < 0.2$ and $0.02 < x < 0.2$, $\text{CaR}_{4-(x+y+z)}\text{Yb}_y\text{Nd}_z\text{Ho}_x(\text{SiO}_4)_3\text{O}$ - only a few exploratory samples made.

Sections 3.2 and 3.3 discuss in detail the material characteristics and spectroscopy of these samples.

3.1.1.2 Crystal Growth

We have emphasized development of a broad understanding of the relationships of such parameters as melt composition and pull rate to the homogeneity of crystals grown during the early stages of this program. For this reason only small crystals suitable for microscopic analysis or transmission spectroscopy have been grown to date (one exception was a one inch rod suitable for laser testing, Table I). Also we have made no attempt as yet to refine our pulling apparatus to produce high optical quality crystals; this will follow in later stages of the program.

The crystal pulling apparatus used for growth of both SOAP and FAP is that described by Mazelsky, Hopkins and Kramer.⁽⁵⁾ The melt is contained in an iridium crucible and induction heated by power from a 10 kHz, 30 kW motor-generator. Temperature control in the case of FAP growth is maintained by feeding the output of a sapphire light pipe detector into an L&N AZAR recorder-controller. The AZAR recorder is coupled to a Norbatrol linear power controller which excites the field of the motor generator. At the high temperatures required for successful growth of SOAP we found it advantageous to replace the light pipe sensor with a pick-up coil which directly monitors the voltage of the work coil. The output of the pick-up coil, suitably converted, is then fed into the AZAR as before.

The design of the pulling furnace, Fig. 1, used for all preliminary studies on this program is a modification of that used for growing laser crystals of FAP:Nd.⁽⁶⁾ As the figure indicates, zirconia refractories

Dwg. 861A228

A

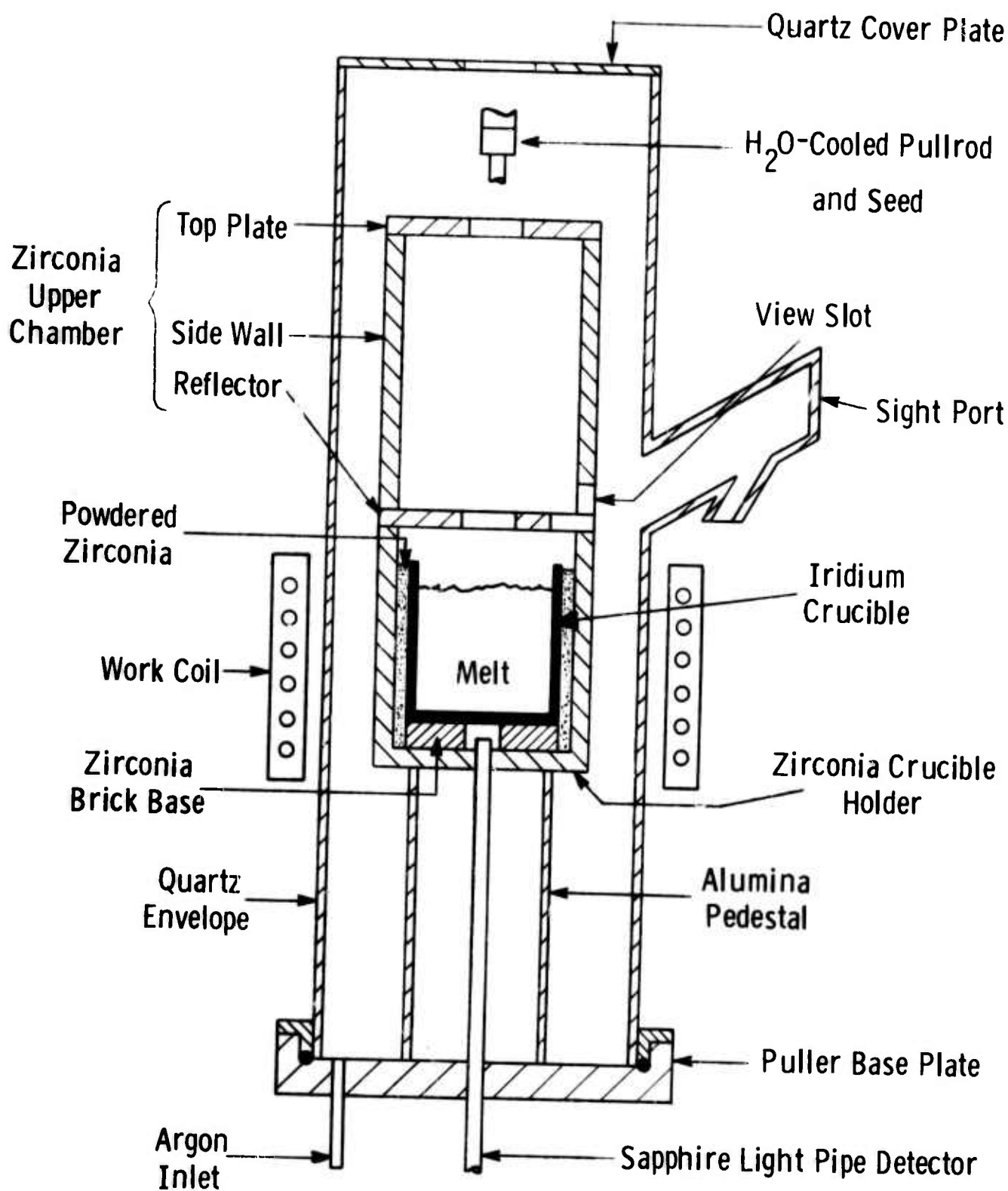


Fig. 1--Section view of crystal growing furnace (schematic)

have been utilized throughout because of their excellent stability at high temperatures.

The need for uniform crucible insulation and a relatively low temperature gradient along the crucible wall when growing SOAP cannot be overemphasized. Failure to observe these requirements may lead to catastrophic crucible failure through localized melting. The upper chamber of the furnace serves to maintain the temperature of the crystal fairly uniformly throughout the cooling of larger boules.

During a growth run, raw materials, prepared as described in the previous section, are charged into the crucible and melted down until the crucible is about three-fourths full. A seed, previously fabricated, is slowly dipped and equilibrated in the melt. Crystals are then generally pulled at rates between 0.06 and 0.15"/hr with the rotation rate between 60 and 80 rpm. Seeds oriented in both the "c" and "a" directions have been used so far although crystals pulled in the latter orientation were generally so poor that further work on this orientation has been held in abeyance. All pulls are carried out in a flowing argon atmosphere. At the termination of a run the furnace is slowly cooled to room temperature.

3.1.1.3 Methods of Sample Analysis

Polycrystalline SOAP samples were routinely analyzed by optical microscopy. A small portion of each melt was ground and sieved. The (-230 + 325) mesh fraction was then mounted on a glass slide in immersion oil and examined with a petrographic microscope for homogeneity and the presence of secondary phases or contaminants such as

iridium oxide. Debye-Scherrer x-ray photographs of selected samples were taken using Ni-filtered, CuK α radiation to confirm the existence of the apatite structure.

Petrographic examination was also performed on longitudinal sections of pulled single crystals. The crystals were polished for microscopic examination by use of wet abrasive papers and by diamond paste. In this manner we were able to observe the effects of variation in composition or pull rate on the quality and homogeneity of single crystal material.

Etch pit techniques can often be used to show the dislocation density and distribution in single crystal laser materials⁽⁷⁾ so we attempted to establish chemical polishes and etches for the various SOAP's. We had only slight success. LaSOAP can be chemically polished with a eutectic mixture of NaF-KF by sample immersion at temperatures between 850 and 950°C. Any excess flux adhering to the polished crystal was later removed by dissolution in boiling water. Treating the polished crystal with aqua regia produced well-defined etch pits similar in shape and distribution to those found in pulled FAP⁽⁷⁾ (see below). No suitable reagents were found for YSOAP or GdSOAP.

3.1.2 Material Characterization

3.1.2.1 Melt Samples

Three types of grains were observed in polycrystalline SOAP samples studied microscopically: type I, optically clear SOAP crystallites (predominant); type II, similar to type I but containing elongate inclusions; and type III, very fine-grained particle masses, brown or black in color,

and translucent to opaque. We interpret type II grains as resulting from crystallization of off-composition melts with subsequent entrapment of impurity liquid in the apatite phase as it crystallizes. Type III grains seem to stem from melt contamination by the crucible material. Distinct brown coloration has been noted especially in samples solidified with a low rate of argon flow through the system. Usually the volume percentage of type II and type III grains was 1-4% but in occasional samples it became much higher. Heavily contaminated samples were discarded and a new sample of the same composition prepared.

We noted significant differences in sample purity between different SOAP:Ho varieties. The YSOAP:Ho samples were invariably the most pure while those of LaSOAP were the least pure. GdSOAP was intermediate. The same general observation also holds for the doubly and triply doped materials. We reached a similar conclusion regarding the quality of the various SOAP single crystals grown; this is discussed in the next section.

3.1.2.2 Single Crystals

We have made preliminary studies of the broad effects of crystal composition, pull rate, seed orientation, and diametral uniformity upon the quality of pulled SOAP crystals. The initial compositions investigated were chosen on the basis of their relatively high fluorescence brightness in spectroscopic tests or their usefulness for transmission measurements. Table I lists the crystals grown to date, growth conditions employed, pertinent observations with respect to crystal quality, and the use to which the crystal was put.

TABLE I - PRELIMINARY SOAP CRYSTAL GROWTH DATA

| Crystal Number | Composition | Pull Rate (in/hr) | Growth Axis | Observations | Use |
|----------------|---|-------------------|-------------|---|---------------------------|
| <u>YSOAP</u> | | | | | |
| 132-202867 | CaY _{3.9} Ho _{.1} (SiO ₄) ₃ 0 | 0.1 | c | somewhat cloudy | transmission measurements |
| 6-203380 | CaY _{2.9} Er ₁ Ho _{.1} (SiO ₄) ₃ 0 | 0.15 | c | many tubular inclusions along growth direction, weak striations, cracked-too rapid broadening | microscopic examination |
| 14-203380 | " | 0.145 | c | - | seed material |
| 9-203380 | " | 0.10 | c | tubular and globular inclusions striations, small IrO ₂ inclusions | microscopic examination |
| 11-203380 | " | 0.08 | c | few globular inclusions mainly near seed striations | transmission measurements |
| 16-203380 | CaY _{2.9} Er _{.9} Tm _{.1} Ho _{.1} (SiO ₄) ₃ 0 | 0.1 | c | inclusions mainly at seed heavily striated | transmission measurements |
| 18-203380 | " | 0.11 | c | globular inclusions in top section | laser rod |
| 113-202867 | " | 0.06 | a | very cloudy, fine inclusions throughout low angle grain boundaries | microscopic examination |
| 90-203381 | CaY _{3.8} Tm _{.1} Ho _{.1} (SiO ₄) ₃ 0 | 0.1 | c | globular inclusions | transmission measurements |
| 92-203381 | " | 0.15 | c | - | seed material |
| <u>LaSOAP</u> | | | | | |
| 60-203381 | CaLa _{3.9} Ho _{.1} (SiO ₄) ₃ 0 | 0.1 | c | few tubular and globular inclusions | microscopic examination |
| 154-202867 | CaLa _{2.9} Er ₁ Ho _{.1} (SiO ₄) ₃ 0 | 0.15 | c | milky, heavy bands of inclusion parallel to solid-liquid interface | " |
| 94-203381 | CaLa _{2.9} Er _{.9} Tm _{.1} Ho _{.1} (SiO ₄) ₃ 0 | 0.08 | c | scattered globular inclusions | transmission measurements |
| <u>GdSOAP</u> | | | | | |
| 52-203346 | CaGd _{3.9} Ho _{.1} (SiO ₄) ₃ 0 | 0.15 | c | inclusions at seed end | microscopic examination |
| 54-203346 | " | 0.15 | c | inclusions at seed end cracked-too rapid broadening | " |

The most common defects we observed in "c" crystals of pulled SOAP were second phase inclusions. As would be expected this type of defect is most obvious at high growth rates⁽⁶⁾ where rejected solute has insufficient time to diffuse from the solid-liquid interface.

Figures 2 through 4 illustrate the various types of inclusions observed in YSOAP crystals examined microscopically. At higher growth rates inclusions are generally elongated in the growth direction, Fig. 2, due to migration of the entrapped solute along the axial temperature gradient present in the growing crystal.⁽⁸⁾ When Er and Tm are present inclusions are not only elongated but are often haloed by a ring of secondary phase, Fig. 3. The reason for the halo is not clear but it may represent a reaction of the entrapped liquid with the apatite matrix. The phase relationships in this system are undoubtedly quite complex especially when two or three doping elements are present in the host.

As the growth rate is reduced, both the morphology and distribution of the inclusions change. Particles become much smaller and more globular in character, Fig. 4. At rates near 0.08 in/hr second phases were nearly eliminated from YSOAP except in regions where diameter changes were rapid, e.g., during seeding. Over-rapid broadening often leads to crystal fracture with the majority of cracks initiating on second phase particles entrapped during the transient growth stage (Fig. 2).

Prior experience had indicated that crystals pulled parallel to the "a" axis were usually very poor and so most of our work has centered upon "c" crystals. We did, however, examine one "a" crystal microscopically. The crystal contained copious low angle boundaries



Fig. 2--Elongated second phase inclusions commonly found in YSOAP crystals pulled at high rates. Dark areas are shadows of cracks nucleated at the inclusion-matrix interface. Growth direction vertical. Transmitted light, 100X.

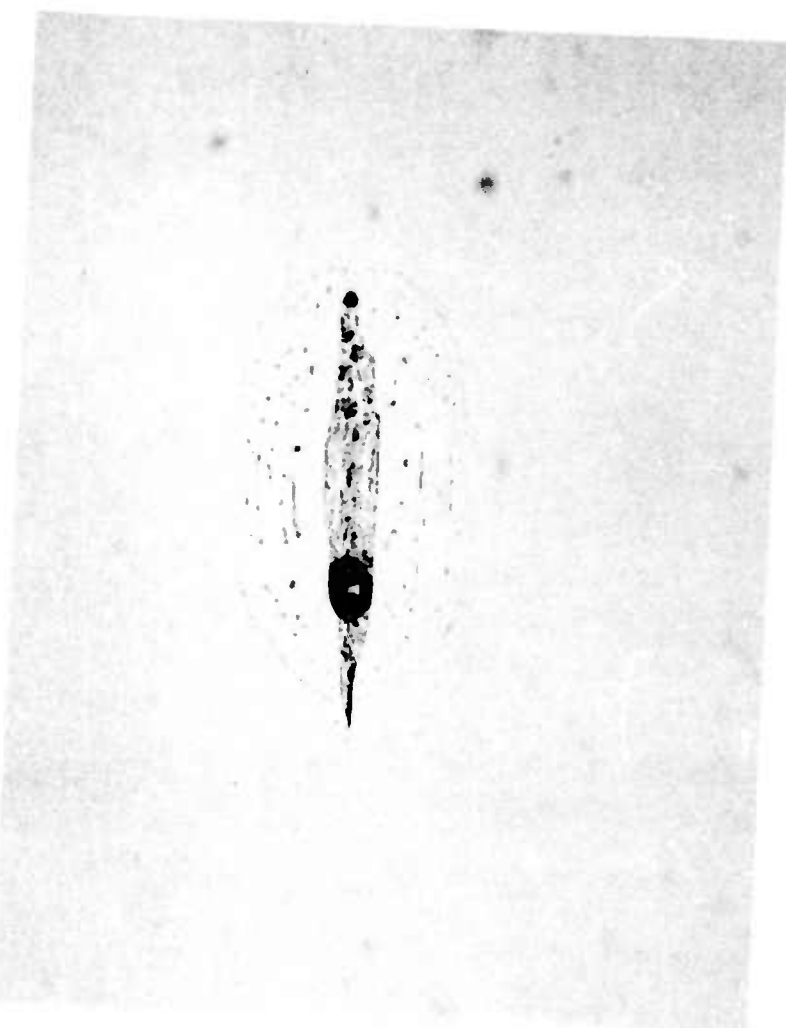


Fig. 3--Haloed inclusions observed in heavily sensitized YSOAP crystals.
Growth direction vertical. Transmitted light, 500X.

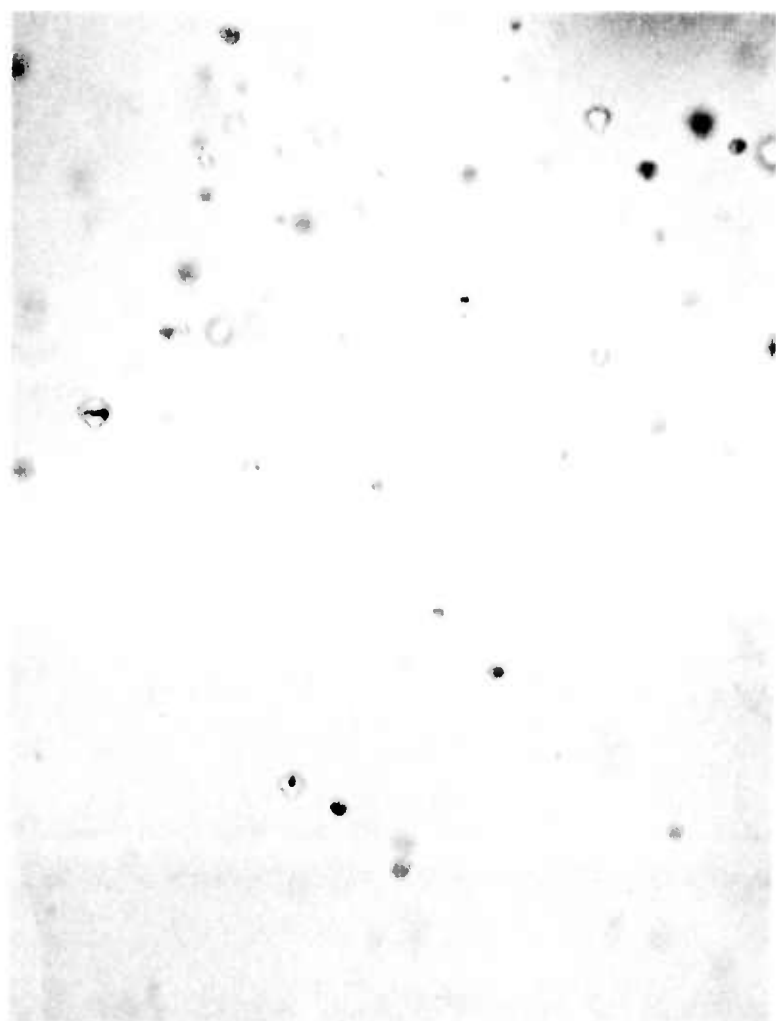


Fig. 4--Globular inclusions developed in YSOAP crystals at slower pull rates. Growth direction vertical. Transmitted light, 200X.

lying approximately parallel to the basal plane of the apatite structure, Fig. 5. Most "c" crystals are relatively free of such boundaries. This boundary structure is apparently the same as that previously noted in "a" axis FAP crystals.^(6,7) Although it is not obvious at the magnification employed in Fig. 5, the boundaries are decorated by a fine network of second phase particles rendering the crystal nearly opaque. Under certain conditions low angle boundaries and dislocations in FAP can be decorated in a similar fashion by a second phase, $\text{Ca}_3(\text{PO}_4)_2$.⁽⁹⁾

The only other notable observations pertinent to the crystal growth of YSOAP were: (1) the occasional presence of small ($< 5\mu$) size iridium oxide particles in pulled crystals and (2) the heavily striated nature of crystals grown from melts containing a high erbium content. We feel the seemingly random occurrence of iridium oxide in crystals is probably due to poor atmosphere control in some runs and can, therefore, be eliminated. Striations, which represent variation in dopant concentration at somewhat regular intervals along the crystal,⁽⁶⁾ are more inherent features of the growth process itself. These bands are parallel to the solid-liquid interface and may stem from convection in the melt.⁽¹⁰⁾ Striations can perhaps be reduced in intensity by decreasing the temperature gradient in the liquid which we consider is an unnecessary refinement in technique at this time.

The trends discussed above with respect to growth of YSOAP apply in general to LaSOAP as well. Reduced growth rate, uniform crystal diameter, small amounts of doping and "c" axis seeds all improve the general crystal quality of LaSOAP. However, we noted that in all cases

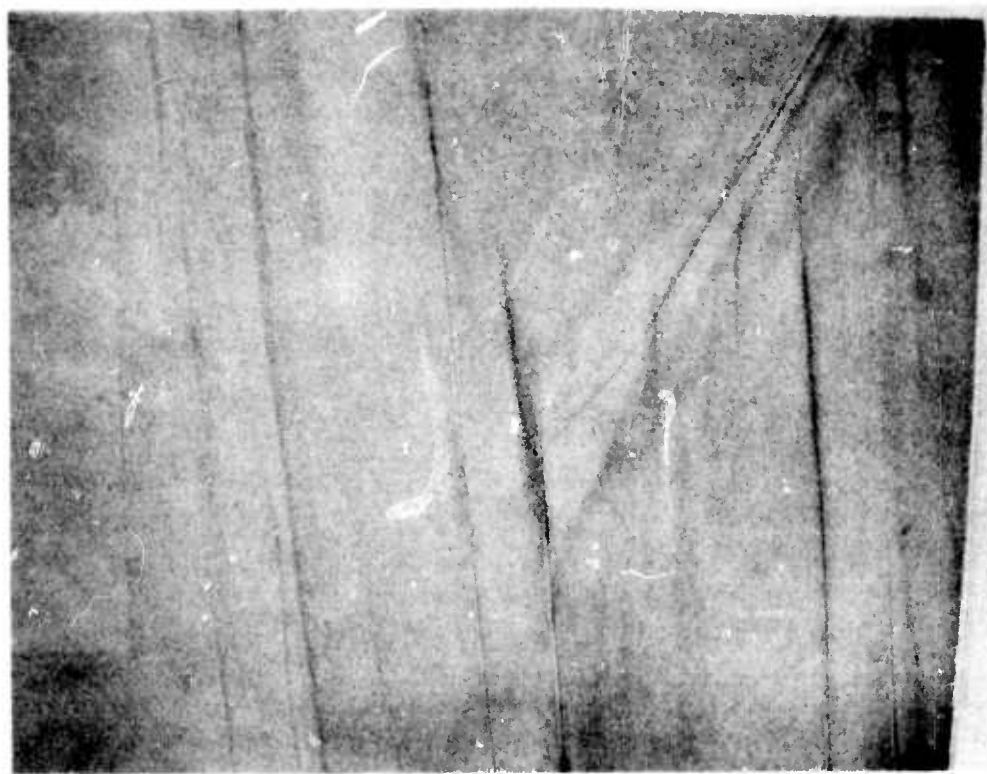


Fig. 5--Precipitate-decorated low angle boundaries in an "a" crystal of sensitized YSOAP. Growth direction normal to plane of paper. Transmitted light, 200X.

when analogous compositions and pull rates were employed, LaSOAP crystals were always of poorer quality than the corresponding YSOAP crystals. All LaSOAP crystals examined contained copious inclusions. This result is perhaps not unexpected since the atomic radii of the dopant, Ho, and the most interesting sensitizers, Er and Tm all lie within the range 0.87-0.91 Å and therefore provide a much better size match when substituted for Y (atomic radius, 0.92 Å) than for La (atomic radius, 1.14 Å).

We conducted relatively few studies on the growth of GdSOAP. Crystals grown at high rates contained inclusions mainly at the seed-crystal junction (Table I). GdSOAP was eliminated from further study on the basis of its poor spectroscopic properties which are discussed in Section 3.2.

Figure 6 illustrates the distribution of etch pits found on the longitudinal section of a LaSOAP "c" crystal. We made only a cursory examination of the dislocation structure in the crystals, but based upon these observations we feel that dislocation arrays in SOAP crystals will be very similar to those discovered in pulled FAP crystals.^(6,7)

3.1.3 Conclusions

From our materials preparation and growth studies we reached the following conclusions:

1. Polycrystalline SOAP samples, as in the case of FAP, provide a fast and reliable method to survey a large number of compositions for subsequent spectroscopic analysis.
2. Microscopic analysis of polycrystalline and single crystal samples of SOAP show that YSOAP is always more homogeneous and free of

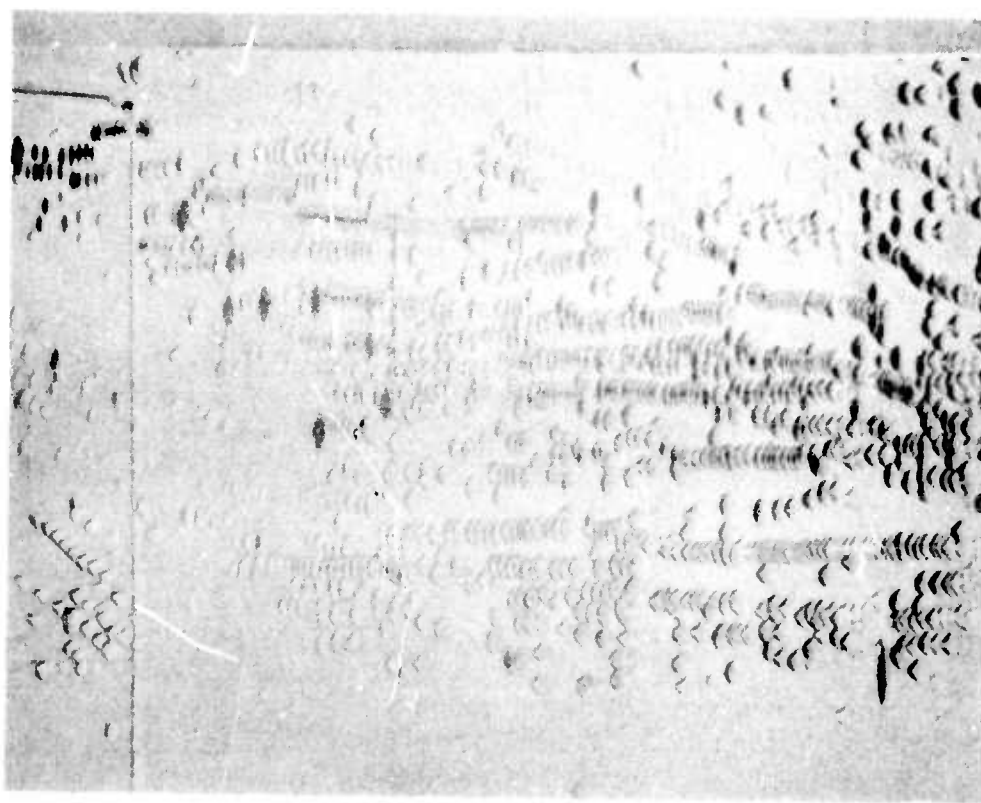


Fig. 6--Etch pits delineating low angle boundaries in a chemically polished crystal of LaSOAP. Growth direction undetermined. Reflected light, 200X.

inclusions than analogous La or GdSOAP compositions prepared under the same conditions. Since LaSOAP offers no distinct advantage with respect to spectroscopic properties, we recommend that it be dropped from further study on this program.

3. Reduction in pull rate and maintenance of uniform crystal diameter tends to suppress inclusion formation in SOAP crystals. This also reduces the tendency to crystal fracture.

4. Crystals containing high percentages of dopant and sensitizers are striated parallel to the solid-liquid interface.

5. Pulling parallel to the "a" axis of SOAP generally results in crystals of poor quality since such crystals contain a fine dispersion of second phase particles entrapped along low angle basal plane boundaries.

3.2 Optimization

3.2.1 Optimization of Rare-Earth Sensitized SOAP

The determination of the best laser composition among the rare-earth-doped SOAP compounds is a more difficult problem than the problem of optimizing, say, FAP:Ho,Cr. To begin with, there is more than one SOAP host to be considered. Once the best host is determined from spectroscopic data, there is the problem of determining the optimum concentrations of three or more independently variable rare-earth ions. Assuming this is done to a satisfactory degree from spectroscopic measurements there still remain three important considerations, any of which can effect changes in host or composition. The first and most important is the ability to grow single crystals with reasonable ease and in suitable quality. The second deals with energy transfer considerations.

Since the point of sensitization is to provide better laser efficiency, there is only a limited value to a composition in which energy is transferred too slowly to do any good. Such a material might appear to be good in steady state fluorescence measurements, and may be suitable for CW laser applications, but it could be poor in pulsed operation. Finally, there remain the results of laser tests, where, because of pumping considerations, the deciding factors are often determined by the need for minimum or maximum optical densities of certain absorption lines rather than transfer yields or quantum efficiencies. It is obvious, that a final determination of the best laser composition cannot be made on the basis of spectroscopic or static measurements alone. Nevertheless, considerable progress can be made in that direction. As evidence of this, we note that the first SOAP:Ho sample which was deduced from spectroscopic data to be worth fabricating into a laser produced laser oscillations with a threshold of 30 joules at 77°K.

In this first portion of the contract period, the emphasis was placed on determining the best SOAP host of the three under consideration, and an approach to determining the best combination of sensitizers and their concentrations. Most of these determinations were made on the basis of spectroscopy, although appropriate attention was devoted to the growth of single crystals. Because of the difficulty of determining the optimum concentration when dealing with three rare-earth ions simultaneously, the studies proceeded in stages, considering first rare-earth ions two at a time, then adding the third rare earth.

3.2.2 Determination of the Best Host

Three hosts were initially considered in the SOAP family. These were the Y-, La-, and GdSOAP. In addition, a fourth host appears inadvertently when high Er concentrations are used. Er-doped SOAP behaves as though it were a different host when the value of x exceeds 2 in the formula $\text{CaR}_{4-x}\text{Er}_x(\text{SiO}_4)_3\text{O}$.

The determination of the best host began by considering the properties of Ho in each of the SOAP compositions without benefit of sensitizers. The rationale was that a host in which an activator behaved well alone was likely to be more suitable than one in which an activator behaved poorly by itself. This criterion turned out to be justified. The worst host for Ho alone was GdSOAP. Subsequent additions of sensitizers, though beneficial, failed to bring the brightness of this material up to the values obtained for the Y- and LaSOAP's.

Figure 7 shows some typical results of relative fluorescence brightness measurements obtained with each of the SOAP hosts in question, for varying Ho concentrations. The La- and YSOAP's are virtually undistinguishable as far as relative brightness of unsensitized Ho is concerned. There is very little evidence of concentration quenching at these concentrations, and the initial rise at very low Ho concentrations is simply accounted for by insufficient Ho to provide complete absorption of the incident excitation. The GdSOAP, on the other hand, gave a relative brightness curve that is a factor of ten lower than that for La and Y, and which shows evidence of a rather early onset of concentration quenching. (There is an insufficient range of Ho concentrations to

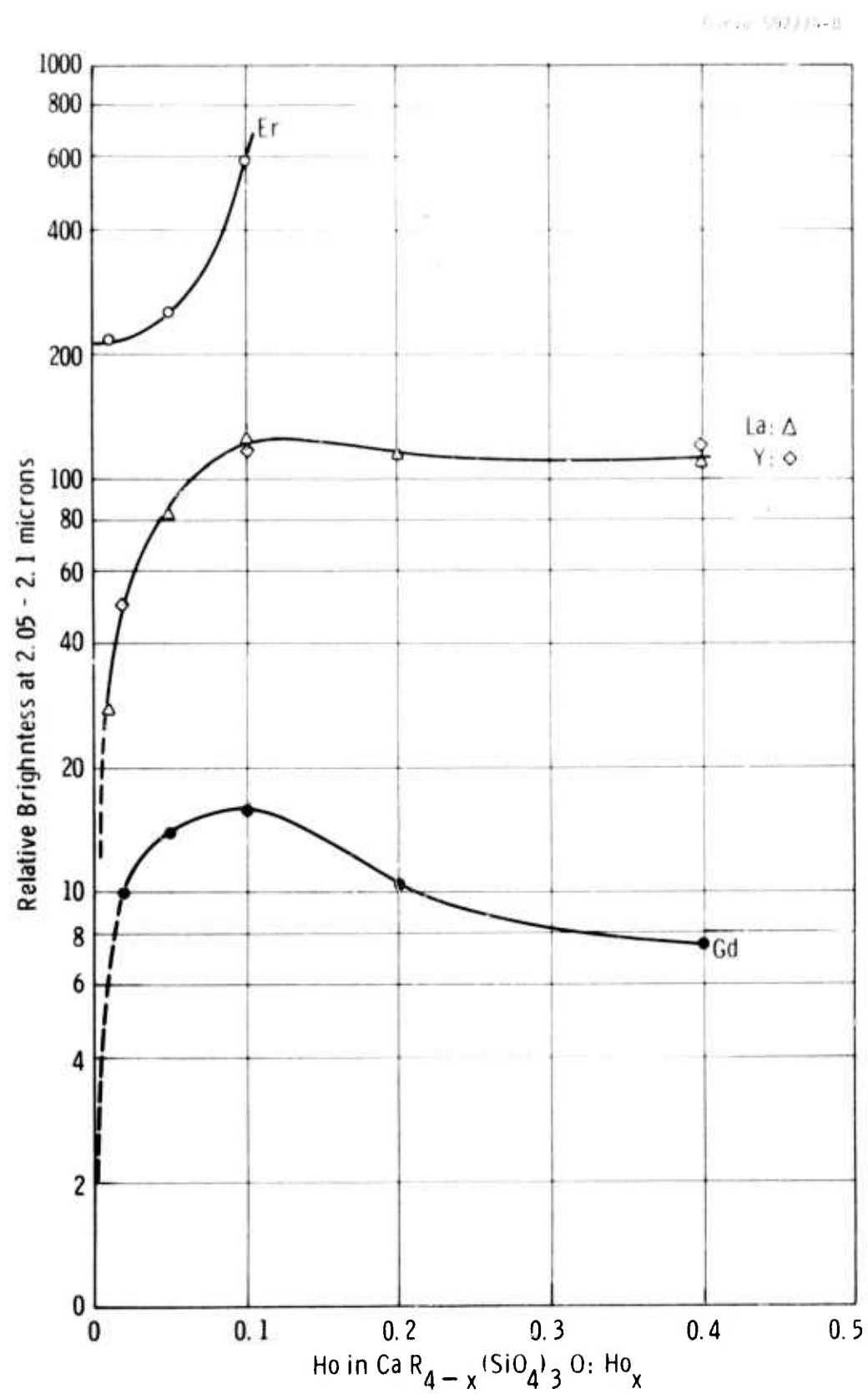


Fig. 7--The dependence of the $^5I_7 \rightarrow ^5I_8$ fluorescence intensity on Ho^{3+} concentration in SOAP hosts of different compositions.

determine the extent of concentration quenching present.) The brightest samples were those of ErSOAP, and they exhibited a superlinear dependence of brightness on Ho concentration. This was not unexpected, since Er is known to sensitize Ho, and the transfer efficiency of a sensitizing-activator combination increases rapidly with an increase in the concentration of the activator. The ErSOAP will not be considered further in this section, but will be discussed in conjunction with sensitizers for Ho.

The results with the GdSOAP tended to rule out this material as a laser host for Ho. Before doing so, however, some samples analogous to those for La- and YSOAP were studied containing sensitizers for Ho. The object was to make sure that our initial bases for rejecting the GdSOAP were well founded. As it turned out, sensitized Ho samples of GdSOAP were consistently a factor of ten or more poorer than comparably doped Y- or LaSOAP's. The poor behavior of the GdSOAP is somewhat unexpected, in view of the fact that Gd^{3+} is devoid of energy levels between the ground state and $32,000\text{ cm}^{-1}$ ($\sim 310\text{ nm}$). We have made no effort up to the present time to determine the reason for this poor behavior, but the possibility that other rare-earth impurities may be responsible cannot be ruled out. Regardless of the reason, GdSOAP was eliminated from further consideration as a host.

The choice between LaSOAP and YSOAP was made later, in favor of the YSOAP. The determining factors were the superior brightness of the YSOAP samples when rare earth sensitizers were added, the tolerance of YSOAP for higher rare-earth concentrations, and the relatively better quality of the sensitized YSOAP samples.

3.2.3 Transfer Considerations

In using sensitization as a means for enhancing the efficiency of a laser, certain basic requirements must be kept in mind. These include efficient absorption of pump radiation, efficient transfer of absorbed energy, and efficient activator fluorescence. In addition there may be an upper limit on permissible transfer times in certain instances, for example where pulsed operation is required. The basic energy transfer mechanisms have been well formulated by Dexter,⁽¹¹⁾ and Dexter's work generally provides the basis for understanding most of the problems encountered in sensitization. There still remain individual problems to be considered. This is especially true of rare-earth ion sensitization, mainly discussed here, and with sensitization by Cr³⁺.

A basic feature of energy transfer is the need for an overlap in the energies of the electronic transitions in the ions involved in the transfer process. This overlap is easy to predict in the ions having d-band optical transitions. It is more difficult to predict in transfer between rare-earth ions. In general, the difficulties are due to the narrow absorption and emission lines of rare earth ions, and their generally low transition strengths. The former makes it difficult to obtain good overlap between energy levels of two dissimilar rare earth ions, restricting the use of rare-earth sensitizers to certain specific combinations. The weakness of the transitions generally makes for weak interactions requiring, in many cases, rather high concentrations of rare earth ions for effective sensitization. A further complication is the large number of energy levels within the rare-earth ions. This makes the direction of energy transfer sometimes variable and unpredictable.

The rare earth ions which were considered in greatest detail as sensitizers for Ho^{3+} were Er^{3+} and Tm^{3+} . Both of these ions have been shown to transfer to Ho^{3+} .⁽¹²⁾ In addition, Yb^{3+} , and Nd^{3+} in combination with Yb^{3+} are being considered, since Yb^{3+} is known to transfer to Er^{3+} ,⁽¹³⁾ which in turn transfers to Ho^{3+} . Nd^{3+} transfers to Yb^{3+} , and may therefore be useful in very small amounts, because it has absorption bands which are in desirable regions of the visible and near infrared spectra. More than very small amounts of Nd^{3+} can be harmful where Er^{3+} is concerned since there is a tendency for Er^{3+} to transfer energy back to Nd^{3+} , with a consequent loss of energy which might otherwise be transferred to Ho^{3+} .

The energy levels for all five rare earth ions are shown in Fig. 8. One sees that with the exception of Nd^{3+} , the lowest excited state of all of the ions shown is the $^5\text{I}_7$ manifold of Ho^{3+} , which is responsible for the 2 micron emission of Ho^{3+} . One may therefore expect that the 2 micron emission of Ho^{3+} will constitute the most effective sink for energy being transferred among the ions Ho^{3+} , Er^{3+} , Tm^{3+} and Yb^{3+} . The sole exception is Nd^{3+} , which has still lower lying levels. Therefore Nd^{3+} must be added with caution. It should be noted from Fig. 8 that there are relatively few cases where good overlap exists between levels of the different ions. In most cases, transfer occurs with the assistance of phonons, either emitted or absorbed, to make up the energy difference between the optical transitions. The need for phonon assistance introduces into the transfer process a certain amount of temperature dependence, and makes for somewhat longer transfer times.

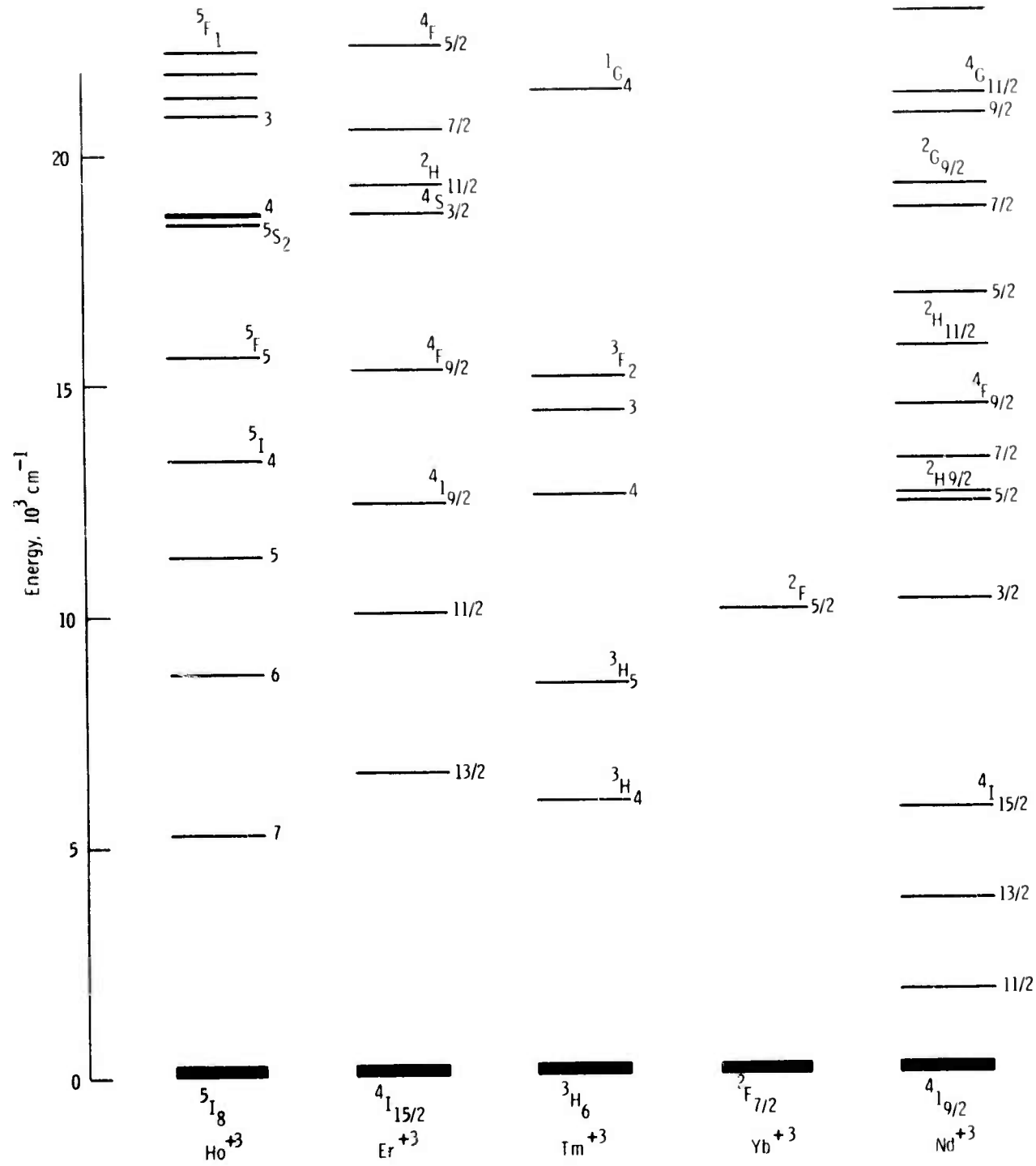


Fig. 8--Energy levels of some selected trivalent rare-earth ions.

It also results in different transfer times for energy absorbed by different sensitizer bands. Since the objective for this initial six-month period was the more general one of determining the best host and the optimum sensitizer and activator concentrations, relatively little time was devoted to more detailed questions such as those just mentioned.

In the following section, we describe in somewhat more detail the optimization of Er+Ho and Er+Tm+Ho in SOAP.

3.2.4 Optimization of Er and Ho in SOAP

The optimization of rare earth ions began with the observation that the brightest unsensitized Ho^{3+} samples contained about 0.1 Ho^{3+} .^{*} Accordingly, this value was taken as the starting concentration of Ho^{3+} . Samples containing various Er^{3+} concentrations ranging from $x = 0$ to $x = 3.9$ (the maximum possible Er concentration) were prepared and compared as to relative brightness under reproducible conditions. Subsequently, similar series of Er samples were made with Ho concentrations above and below the 0.1 concentration. Excitation was by means of a 800 watt d.c. operated short-arc xenon lamp, filtered through a 10 cm water cell which cut off wavelengths longer than 1.2 microns. In later measurements the water cell was replaced with a filter which transmits to 1.5 microns, thereby providing a better measure of the effectiveness of Er^{3+} . While the spectrum of a d.c. short-arc xenon lamp differs somewhat from that of a pulsed linear xenon lamp, experience has indicated that the similarities in spectra are great enough to make the results

*All rare earth ion concentrations will be given in terms of the value of x in the chemical formula $\text{CaR}_{4-x}(\text{SiO}_4)_0:\text{M}_x$ where M is a rare earth ion.

a valid guide to xenon lamp pumped laser operation. The measurements were performed on an excifluor, described elsewhere,⁽²⁾ and whose general form is shown in Fig. 9. Each set of measurements (usually consisting of less than 5) was accompanied by the measurement of a standard Ho sample taken under the same conditions. Use of a standard Ho sample insured that the entire system was working properly and in proper optical alignment. Over the period of six months the relative brightness of the standard sample did not vary by more than \pm 5%, except when deliberate changes were made on the apparatus. Repeated measurements on the same SOAP samples taken at different times agreed to about \pm 5%. In two instances where the results of particular samples showed large deviations from the expected values, it was found that the fault lay with the samples; these samples were reprepared. Each measurement of relative brightness actually consisted of the measurement of the entire infrared $^5I_7 \rightarrow ^5I_8$ fluorescence spectrum from 1.8 to 2.2 microns, taken at medium resolution ($\sim 50 \text{ \AA}$). The resolution was sufficient to detail the main features of each spectrum; while providing reasonable spectrometer throughput, and enough integration of sharp lines to make brightness comparisons (particularly with YAG) somewhat easier.

Figure 10 shows the results from three series of samples with variable Er concentrations and containing 0.05, 0.1, and 0.15 Ho, respectively. The Er concentrations range from 0 to maximum (3.95 Er in the case of 0.05 Ho, and appropriately less with greater amounts of Ho). The data points are connected by lines mainly to show trends. The data shown is for YSOAP. A striking feature is the presence of two sets of maxima occurring

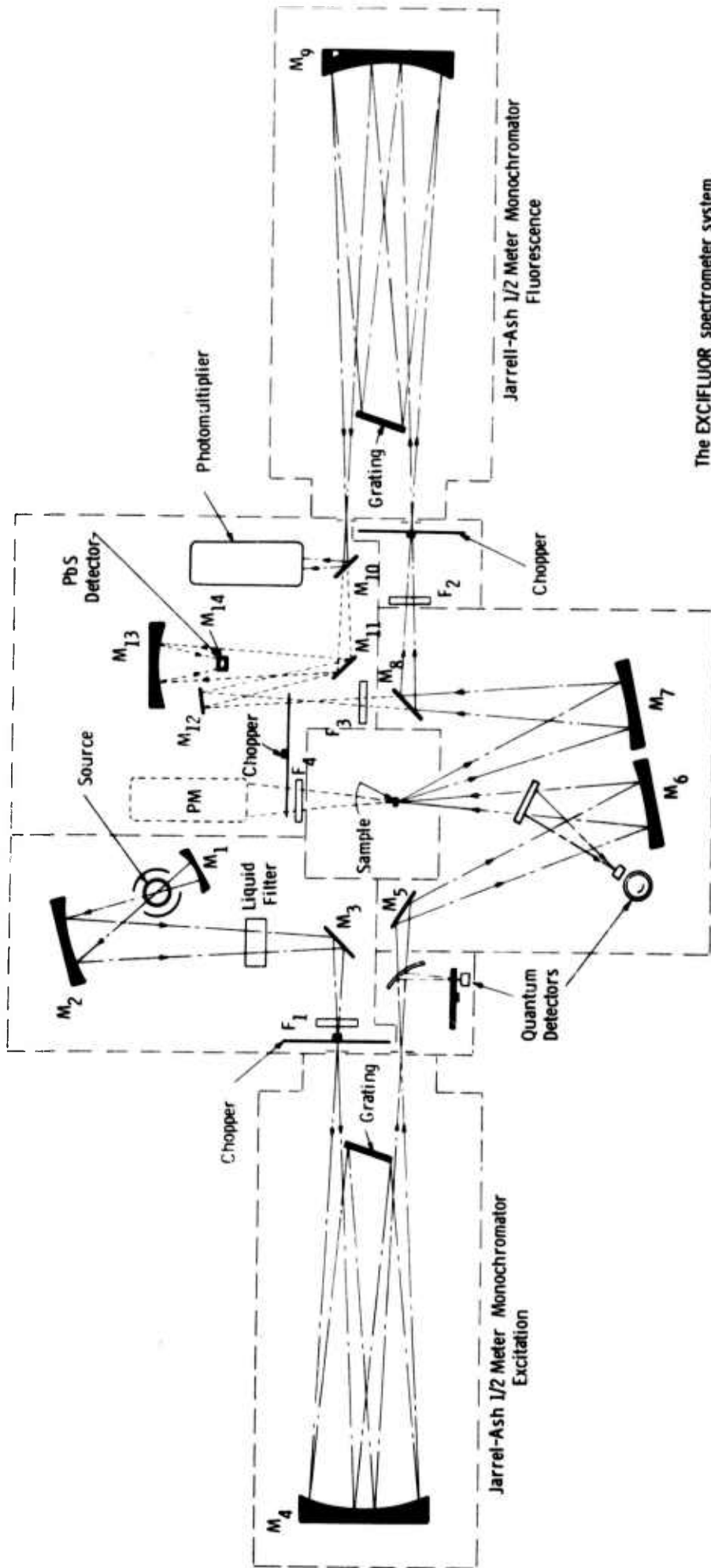


Fig. 9--A schematic of the EXCIFLUOR spectrometer system. The light paths are shown dashed for alternate modes of operation.

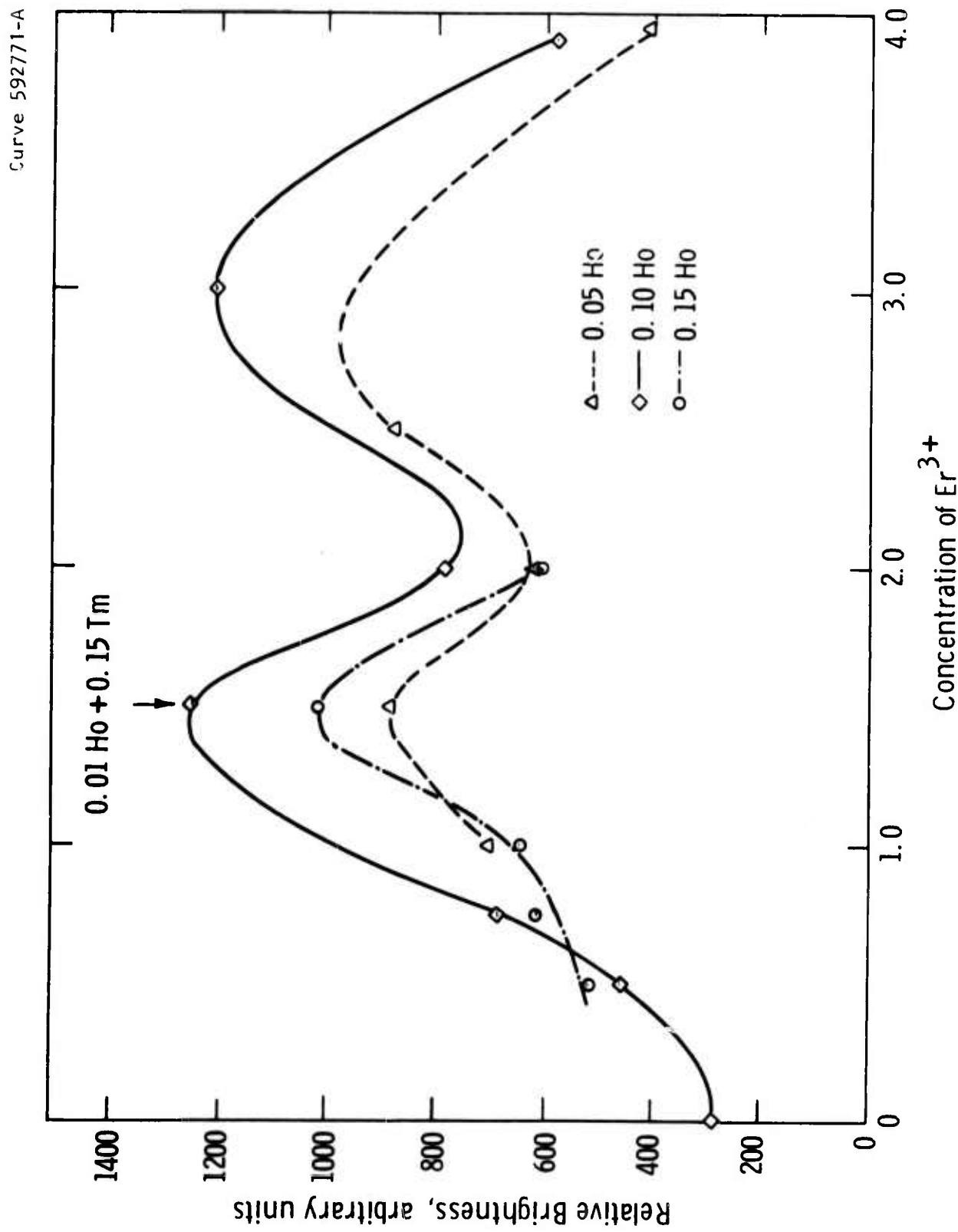


Fig. 10--The dependence of the relative brightness of YSOAP upon Fr concentration. Curves are shown for three Ho concentrations, with lines drawn only to indicate trends.

at the approximate compositions ($Y_{2.5}Er_{1.5}$) and ($Y_{1.0}Er_{3.0}$). The data suggests that we are dealing with two hosts: on the low Er side, the host consists of YSOAP, with Er as a major impurity; on the high Er side, the host may be regarded as predominantly ErSOAP, diluted by a small amount of Y. In order for such behavior to occur, there must obviously be an effect present in addition to simply the sensitization of Ho by Er. This effect must be associated with the host lattice, possibly with the disposition of Ho among the cation sites. The minimum in the brightness curves occurs at equal concentrations of Er and Y. At this composition we can speculate that either there is a high degree of disorder or a superstructure occurs.

Despite the apparent similarity of the brightness data in Fig. 10, the low Er region seemed to yield somewhat higher maximum brightness values than the high Er region. For this reason, and for reasons of economy, the region below Er = 2.0 was chosen for further consideration. Figure 11 shows data similar to that of Fig. 10 plotted in a manner designed to show contours of equal brightness. The emphasis is on the low Er region. One sees a tendency towards closed contours, with a maximum occurring in the region of Er = 1.5, Ho = 0.1. The presence of a second maximum at about 3.0 Er can be seen from the few points indicated.

A similar family of curves were developed for the LaSOAP. The appearance of the curves for 0.1 and 0.15 Ho were very similar to their counterpart in the YSOAP. Minima and maxima occurred at about the same concentration of Er as in the YSOAP's. The major difference is that

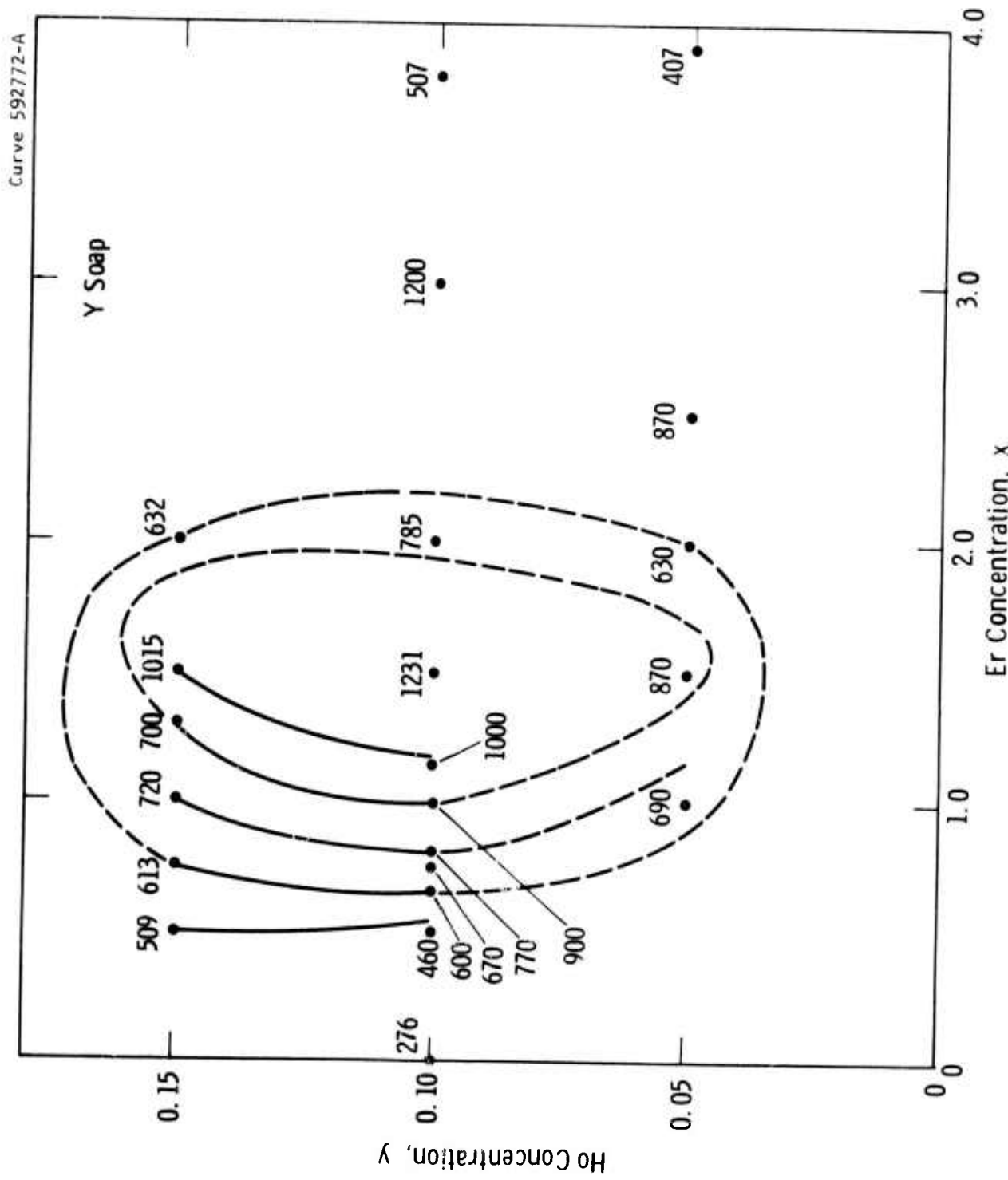


Fig. 11--Equal brightness contour curves for various concentrations of Er^{3+} and Ho^{3+} in YSOAP. Note two regions of brightness maxima.

while the values of brightness at the minima were almost exactly the same as in the YSOAP, the brightness obtained for the peaks of the curves were some twenty percent lower in the LaSOAP's. Subsequent additions of Tm produced substantial improvements in the brightness of LaSOAP's, but their values were still not quite as high as those obtained with analogous YSOAP's. These results, plus the results of crystal growing experiments made us favor YSOAP as the host on which to concentrate our future efforts.

While LaSOAP containing 0.1 and 0.15 Ho behaved quite similarly to the YSOAP with regards to Er concentration, LaSOAP containing 0.05 Ho behaved in an opposite fashion. The brightness was quite low at 1.0 and 3.0 Er, but there occurred a sharp maximum at 2.0 Er, precisely where the 0.1 and 0.15 Ho curves had their minima. In general the behavior of the La- and YSOAP's with respect to Er and Ho concentrations is quite interesting, and deserves some further study, both from the standpoint of understanding the phenomena, as well as for making possible improvements in laser hosts. Unfortunately, the emphasis on eliminating all but the best host, and optimizing the rare-earth concentrations did not permit such a study to be done during this period.

As we mentioned earlier, some measurements were made on GdSOAP containing various amounts of Er and Ho, just to be sure that we were fully justified in eliminating this host from consideration. The results were uniformly much poorer than we obtained with either La- or YSOAP. While the samples which were made were intended to cover a representative region of the total range of possible compositions, no attempt was made to develop curves analogous to Figs. 10 and 11.

3.2.5 Addition of Tm

Tm^{3+} was added in a range of concentrations to SOAP samples containing different concentrations of Ho and Er. The Ho and Er concentrations chosen for Tm addition were those which lay in a cluster about the best value obtained for Ho and Er. Thus, the main Er concentrations chosen were 1.0, 1.25 and 1.5 with some samples less and some more Er than these amounts. Ho concentrations were mainly 0.05, 0.1 and 0.15, with some intermediate concentrations. The results form a three component matrix not easily displayed in a single figure. Figure 12 shows the brightness values obtained for samples containing 0.1 Ho, with several Er concentrations as a function of Tm concentration. One sees that the brightness values do not vary monotonically with Tm concentration, but contain various maxima and minima. The behavior is somewhat reminiscent of the Er-Ho system, but so far, less simple. We are inclined to attribute the behavior of the Tm samples to variations in transfer yield with Tm concentration as far as the Ho emission is concerned. As we mentioned earlier, in Section 3.2.1, energy transfer depends on a coincidence of energy levels between activator and sensitizer. In principle, therefore, energy is transferred in both directions, and generally other considerations determine which way the net transfer yield will occur. Particularly among the rare earth ions, the magnitude and even the direction of transfer can vary quite considerably with concentration. Figure 8 shows the great many possible transfer routes that can occur among the three ions under present consideration, and we are inclined to attribute the observed behavior to such causes as these.

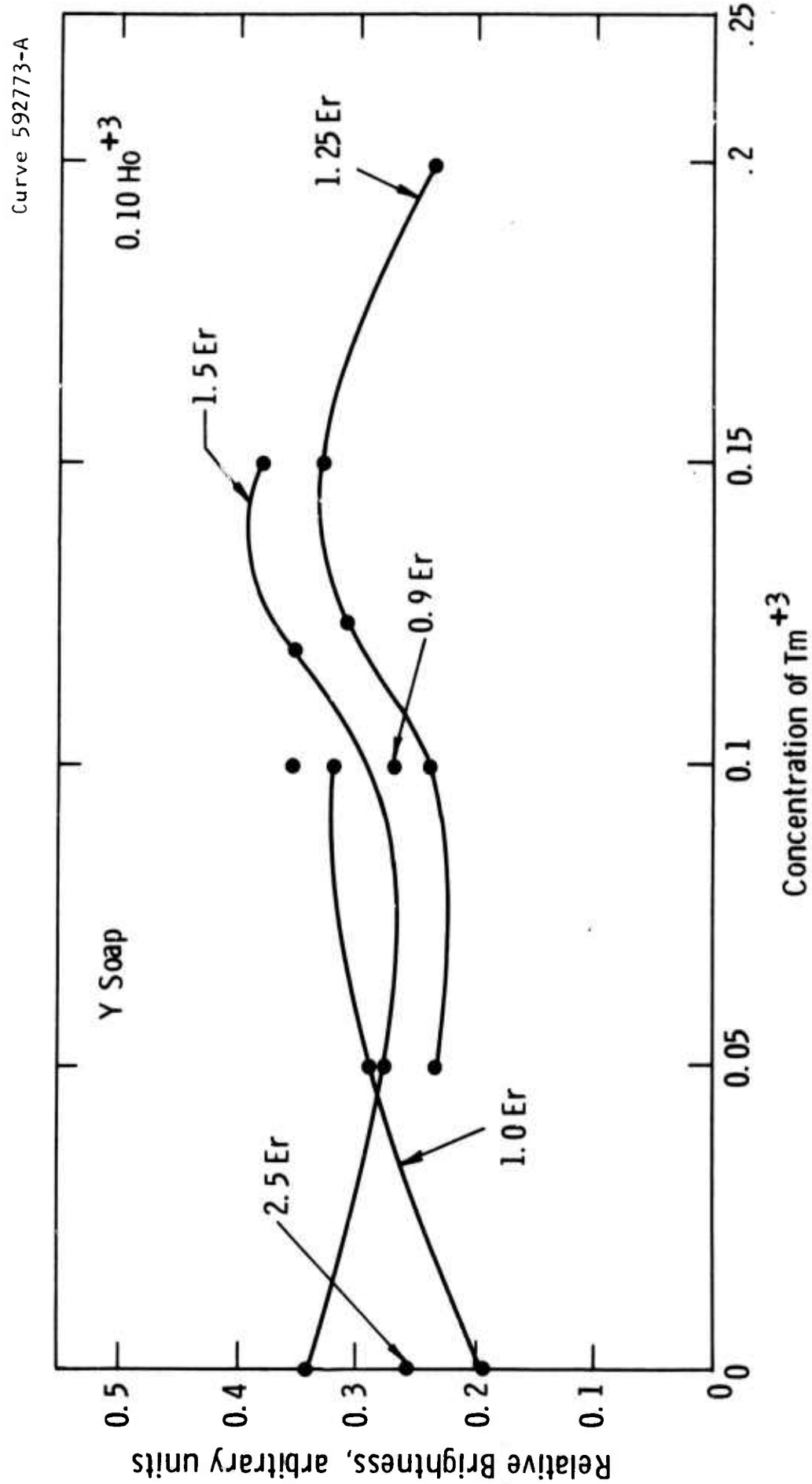


Fig. 12--The dependence of the relative brightness of YSOAP containing 0.1 Ho_{3+} and various concentrations of Tm^{3+} and Er^{3+} .

Partly because of the above possibilities, and partly to be certain that we were really transferring as much of the Er and Tm absorbed energy to Ho, we ran fluorescence measurements in the 1.4 to 1.8 micron range on selected samples, to see if excessive fluorescence of either Tm³⁺ (at 1.8 microns) or Er (at 1.55 microns) occurred. Both Er and Tm fluorescence could be detected in some samples, showing that transfer to Ho was not quite complete. In no case, however was the Er or Tm emission more than 5% of the total fluorescence yield, including Ho, and in the better samples, these losses were insignificant.

Figure 13 shows another set of data to complement that of Fig. 12. Here we show, for one value of Er concentration, values of brightness obtained with different amounts of Ho and Tm. One sees, from both this figure and the previous one, that the maximum improvement in brightness contributed by Tm is approximately 10-20%, with the lower figure applying to the better Er, Ho samples. This is about the enhancement one would expect based on the spectroscopy of these rare-earth ions. Referring to Figs. 10 or 11, we see that the enhancement due to Er is, by way of contrast, a factor of 4 to 6. The comparison is not altogether a fair one. Had the comparison been made as though Er were added to Ho-Tm samples the effect of Tm would have appeared somewhat greater and that of Er somewhat less. Nevertheless the data shows clearly the overriding need for Er as a sensitizer, and the relatively smaller need for Tm. This is in accord with the absorption spectra of these ions.

Based on the foregoing work, the best composition for a laser is CaY_{2.27}Er_{1.5}Tm_{0.13}Ho_{0.1}(SiO₄)₃O. As noted elsewhere, this composition

Curve 592841-A

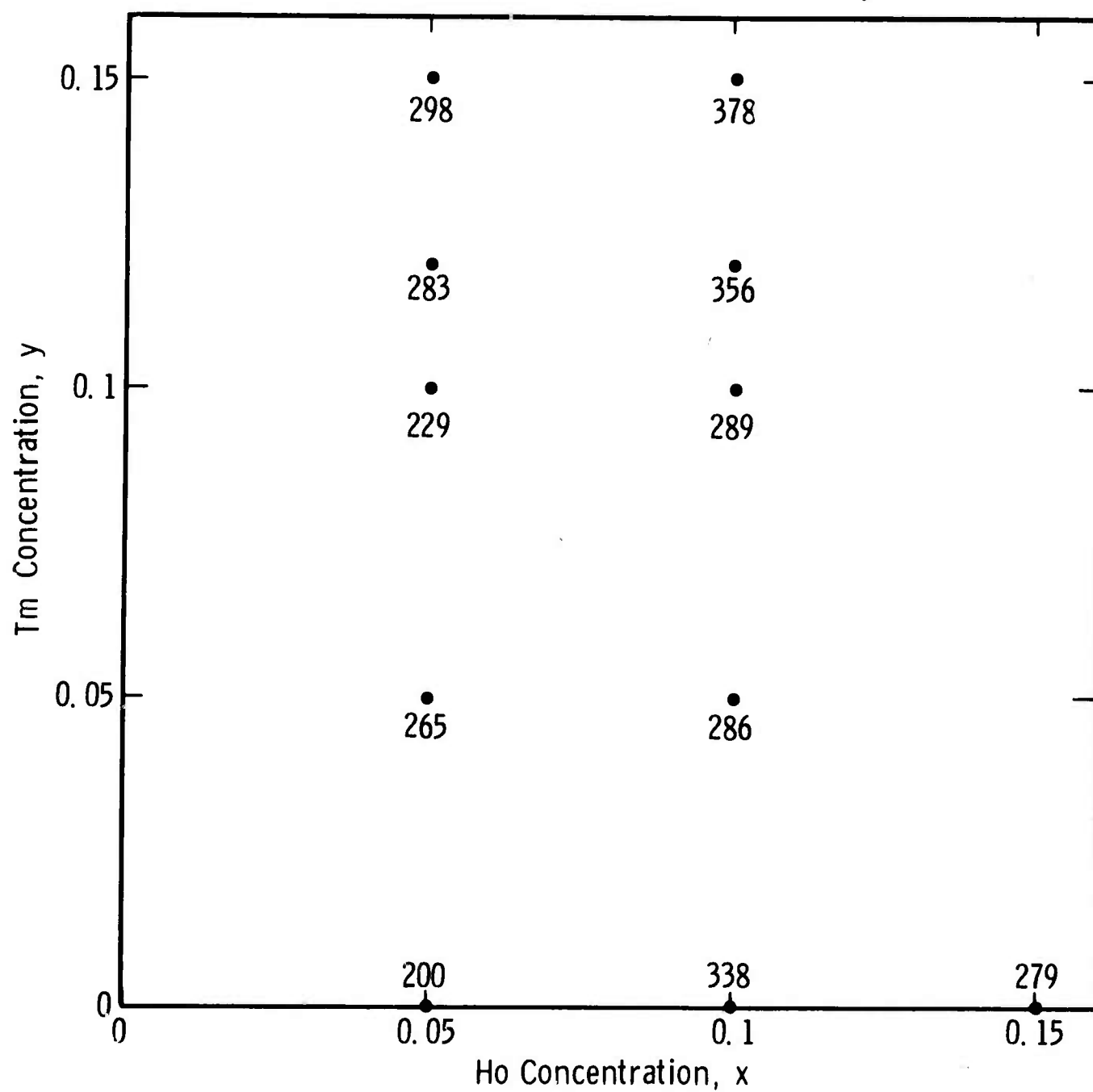
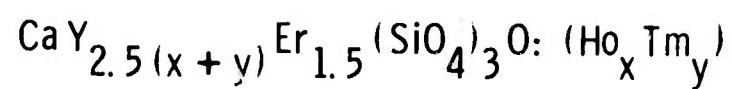


Fig. 13--Relative brightness values for YSOAP containing 1.5 Er^{3+} , and various concentrations of Ho and Tm.

may require some adjustment, based on laser tests, crystal growth considerations, and further spectroscopy. Such changes are not expected to cause the composition to depart greatly from the above formula, however.

3.2.6 Other Sensitizers

Use of the three rare earth ions, Ho, Er and Tm provides fairly good absorption over the region from 0.4 to 1.9 microns. As will be seen in the subsequent sections, the absorption is best at the two ends of this range, and worst, in the region from 1.0 to 1.45 microns. There is also a gap in the 0.8 to 0.95 micron region. Unfortunately, the region where absorption bands are lacking is also the region where tungsten and xenon lamps have their highest outputs. There is much to be gained, therefore, by providing additional sensitizers which absorb at these desired wavelengths and transfer efficiently to Ho, whether directly or through an intermediary ion. It is for this reason that Yb and Nd are being considered. Whether the addition of these ions will do more good than harm remains to be seen. Part of whatever gain may result would have to be offset against the additional difficulties in growing crystals. At the present time, only a few exploratory samples have been prepared, with no measurements to report.

3.3 Optical Measurements

3.3.1 General Considerations

Three basic optical measurements have been performed thus far on the experimental SOAP compositions. These include emission, mainly in the 1.8 to 2.2 micron range, transmission (optical density),

from 0.4 to 2.2 microns, and excitation spectra, from 0.4 to 1.1 microns. In addition to these measurements, some preliminary lifetime measurements were made, which are too few to report here. Most of the samples used were in the form of fused polycrystalline samples prepared for the optimization work. A number of single crystals were grown for transmission measurements, as well as for determining laser crystal growth conditions. Each sample made was measured for its fluorescence spectrum; the more interesting samples are being measured for excitation spectra; and the single crystal samples were measured for their transmission spectra, in addition to the other measurements. The correlations between optical transmission spectra and excitation spectra are particularly interesting and useful since excitation spectra are related to their optical absorption through the quantum efficiency and the transfer efficiency. Most of the emphasis up to now has been on fluorescence measurements in order to obtain the relative brightness data needed to determine optimum compositions. At the present time emphasis has shifted to measurements of excitation spectra. As soon as our excitation measurements are completed, decay times and transfer times will be measured on most, if not all of the samples. Some transfer times will be determined concurrently in time resolved excitation experiments.

The apparatus we have been using for transmission measurements is a Cary Model 14R. This is an automatic recording instrument with adequate spectral range and resolution, very good signal to noise, and excellent stray light characteristics. Excitation and fluorescence measurements are taken on our excifluor (Fig. 9), mentioned earlier

in this report. During this reporting period some changes were made in the optical system which resulted in greatly improved optical performance, particularly in the measurements of fluorescence in the infrared. Changes are currently planned to improve the excitation measurements, particularly in the method of ratio detection, to include a capability for measuring time-resolved excitation-spectra. Just as excitation spectra are related to absorption spectra through the activator fluorescence quantum efficiency and the sensitizer transfer efficiency, so time resolved excitation spectra are related to normal (d.c.) excitation spectra through the activator decay time and sensitizer transfer times. The measurements will permit us to determine individual transfer rates for each of the bands appearing in the excitation spectrum of a given material. They should provide interesting and useful information regarding laser performance.

3.3.2 Fluorescence Emission Measurements

We begin by considering the fluorescence emission of Ho in SOAP. The infrared fluorescence of Ho^{3+} is due to the $^5\text{I}_7 \rightarrow ^5\text{I}_8$ transition (Fig. 8). At room temperature, the fluorescence consists of a very broad band extending from approximately 1.9 to 2.12 microns. Poorly defined maxima are visible at 1.9, 1.975, 2.0, 2.06 and 2.12 microns (Fig. 14). Cooling specimens to 77°K results in a substantial sharpening of the emission lines, as can be seen in Fig. 15 for a sample containing Ho, Er and Tm. The spectrometer resolution at which this data was obtained is 16 Å. The lines are relatively broad, approximately 100-200 Å wide at their half maxima, and comparatively few in number. The width of the lines is in large measure probably due to inhomogeneous broadening,

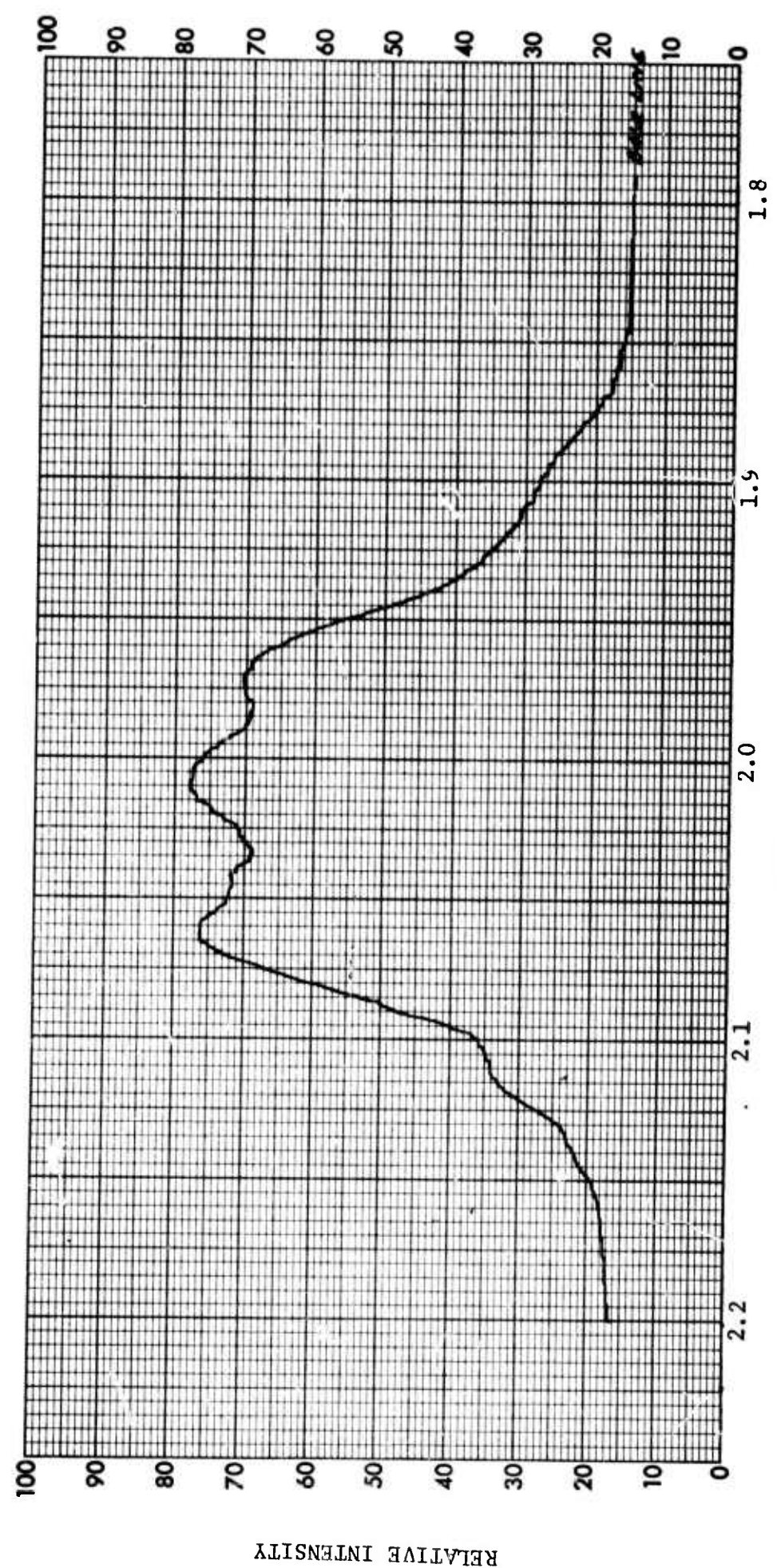


Fig. 14--Room temperature fluorescence of Ho in YSOAP.

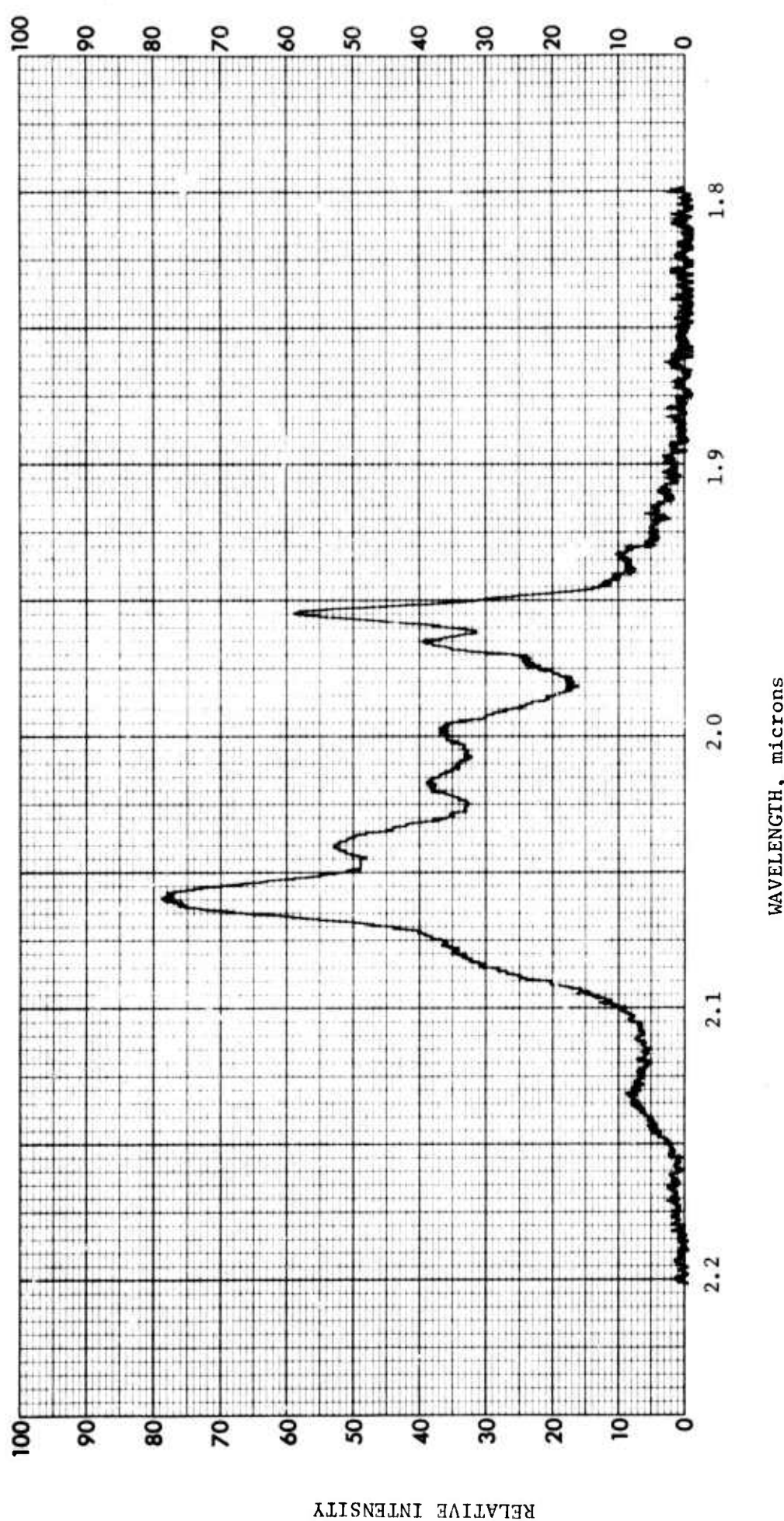


Fig. 15--Fluorescence of Ho in YSOAP at 77°K. (Sample 201720-120-2).

and is not unexpected, in view of our observations regarding the behavior of other rare earth ions in apatites. Some apparent broadening may also be due to the polycrystalline samples used combined with the strong crystalline anisotropy of the apatite structure. Certain of the lines seen in fluorescence appear also in absorption, notably the strong lines at 1.955 and at 2.06 microns. These may be seen in Fig. 16, below. We have not yet attempted to correlate the two sets of spectral data.

3.3.3 Optical Transmission Spectra

Transmission spectra were obtained on a number of single crystals. In general the measurements were intended to identify the properties of the various rare earth ions being used. Figure 16 shows some representative measurements. From the top down they are: the spectrum of Ho^{3+} , of $\text{Ho} + \text{Er}$, and $\text{Ho} + \text{Er} + \text{Tm}$, all present in YSOAP. Similar spectra were obtained on some limited LaSOAP samples. It can be said in general, that the absorption spectrum of Ho in SOAP, as in other hosts, consists of too few lines to be an effective laser ion without benefit of sensitization. This can be seen in the upper panel of Fig. 16. Most of the absorption is confined to the 0.4-0.5 micron region, where it has very limited usefulness for pumping.

Er^{3+} , on the other hand introduces a rather substantial absorption ranging from 0.4 to 1.6 microns, with dominant lines in the region of 0.65, 1.0 and 1.5 microns. These are visible in the center panel of Fig. 16. It is easy to see, by comparing these two panels, why Er is such an effective sensitizer, and why such significant improvements are obtained for Ho with Er. The very strong bands at 1.5 microns are due to the

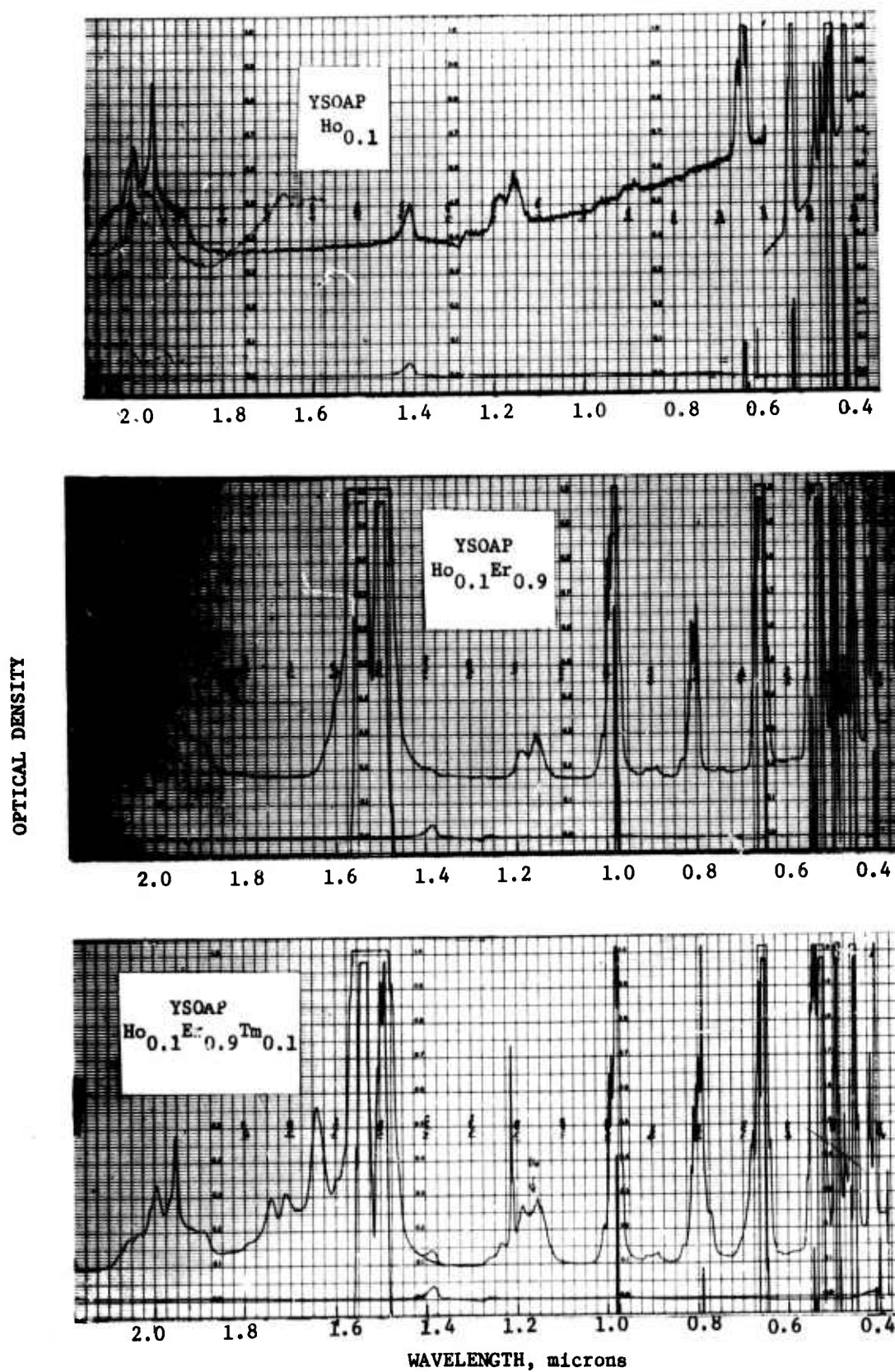


Fig. 16--Optical density of YSOAP single crystals containing 0.1 Ho and different sensitizer combinations as a function of wavelength.
Top panel: Ho alone; center panel: Ho+1.0Er; bottom panel: Ho+0.9Er+0.1Tm. The high sloping baseline in the upper panel is due to scattering by ~ 0.5 micron inclusions. Increasing amplitude is increasing absorption.

$^{4I}_{15/2} - ^{4I}_{13/2}$ transition which produces the 1.5 micron emission in Er.

The effect of adding Tm^{3+} can be seen in the lowest panel of Fig. 16. One can see immediately that Tm adds a number of new lines to the excitation spectra. The more prominent lines are at 0.8 and 1.2 microns, and at 1.65-1.75 microns, just to the long wavelength side of the strong 1.5 micron Er lines. The last mentioned lines are due to the $^3H_6 - ^3H_4$ transition of Tm^{3+} which produces fluorescence at about 1.8 microns and which has produced laser action in several materials. By comparing the lower and center panels one can see that the effectiveness of Tm as a sensitizer falls far below that of Er, and that a 10-20% enhancement due to Tm additions is not surprising. Figure 16 also clearly indicates the spectral regions where additional sensitizer bands would be desirable. These include the region from 1.0 to 1.15 microns, and from 1.2 to 1.4 microns. These regions are particularly important because they are the wavelength regions within which xenon flashlamps and tungsten lamps typically have their maximum spectral radiances. Improved absorption in these regions may be achieved by increasing the Tm content, or, as mentioned elsewhere, by the additions of Yb^{3+} and possibly Nd^{3+} .

3.3.4 Excitation Spectra

As mentioned earlier, excitation spectra are related to optical absorption spectra through the quantum efficiency. They should, therefore, have the same general appearance as absorption spectra, with two exceptions. First, differences in quantum efficiency (or transfer efficiency, if sensitization is occurring) will show up as differences in the amplitudes

of the various excitation lines. Secondly, once pump radiation is essentially totally absorbed in a given line, a further increase in the absorption strength of that line will not result in any further increase in the amplitude of the excitation band corresponding to it. This tends to cause the peaks of lines to appear saturated in excitation, and causes the excitation bands to appear often considerably broader than the corresponding absorption lines because of the greater weight given to the wings of the line. By the same token, detail is often lost in excitation spectra. In general, however, excitation spectra are a more accurate representation of how effectively pump radiation is utilized by a laser material than are the transmission spectra.

Excitation spectra measurements are currently underway for most of the samples that have been prepared. Most of these spectra can be relatively easily related to other data, such as transmission data.

Figure 17 shows three fairly representative spectra of YSOAP containing Ho alone, Ho with Er, and Ho with Er and Tm. These are shown in the same sequence as the corresponding transmission spectra of the preceding figure. Comparing the upper panels of the two figures (Ho alone) we see that, despite the rather dissimilar appearance of the two spectra there is a one-to-one correspondence of the dominant lines. For example, the line at 0.42 microns show up in both spectra; the cluster of lines at 0.45 microns shows up as a broad band with poorly defined structure, but in the same wavelength region; and the lines at 0.54 and 0.65 microns are also seen in both figures. Note, however, that generally the lines look much broader in the excitation spectra, and tend to have more nearly the same amplitudes.

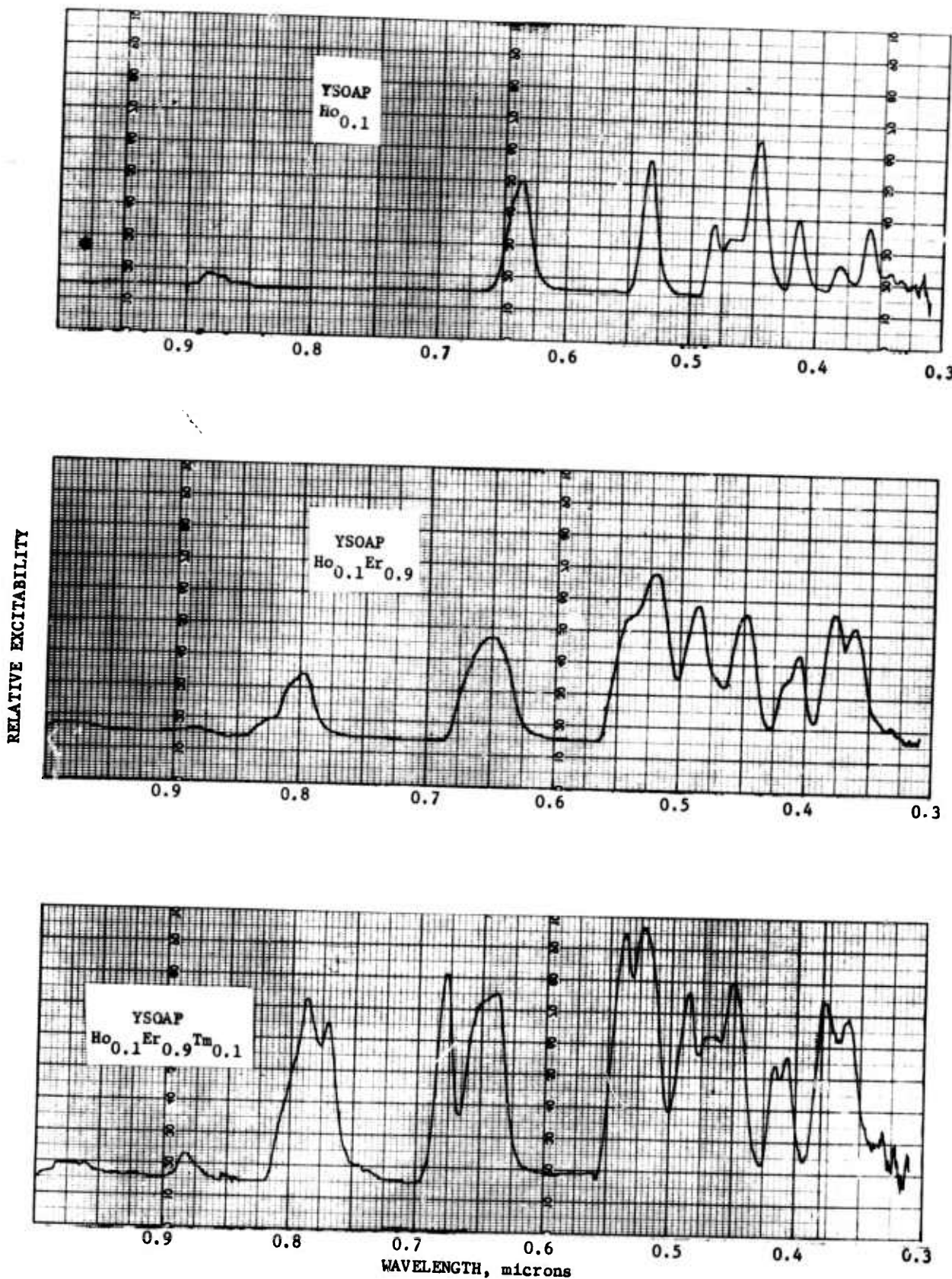


Fig. 17--Excitation spectra of three YSOAP samples having compositions similar to those shown in Fig. 16. Top panel 0.1Ho ; center panel $0.1\text{Ho}+1.0\text{Er}$; bottom panel $0.1\text{Ho}+0.9\text{Er}+0.1\text{Tm}$. Note the distorted shapes of the excitation bands which correspond to different absorption bands.

The center panel of Fig. 17 shows the effect of adding Er to the host. A substantial increase in the excitation bands can be seen particularly at wavelengths shorter than 0.55 microns. A strengthened excitation can be seen at 0.65 microns, as well as a new band appearing at 0.8 microns. Note that the 0.8 micron lines of Er are relatively weak in transmission compared with the lines at shorter wavelengths. In excitation, however, the lines have significant strength. (The transmission curves are in terms of optical density, and therefore also tend to somewhat overemphasize the importance of weak lines.) Note also, that the extremely weak Ho absorption line at 0.9 microns is visible in both excitation spectra.

The lowest panel shows the effect of adding Tm to the host. A new band is evident on the long wavelength side of the 0.65 micron (Er + Ho) band seen in the previous panel. This band is due to a line which appears in the transmission curve as a weak side band to the strong Er lines at .65 microns. The very sharp Tm lines which are seen on the short wavelength side of the 0.8 micron Er lines, are now seen to contribute significantly to the excitation spectra. The region between 0.8 and 1.0 micron is seen even in excitation to need additional sensitizer bands. Unfortunately, in its present form, our apparatus does not permit measurements of excitation spectra to be taken at wavelengths longer than 1.0 micron.

3.3.5 Other Sensitizers

Work on apatites containing Ho sensitized by Cr is just beginning, and relatively little has been done so far, other than some work done prior to the start of this contract. Figure 18 shows the

Curve 590214-B

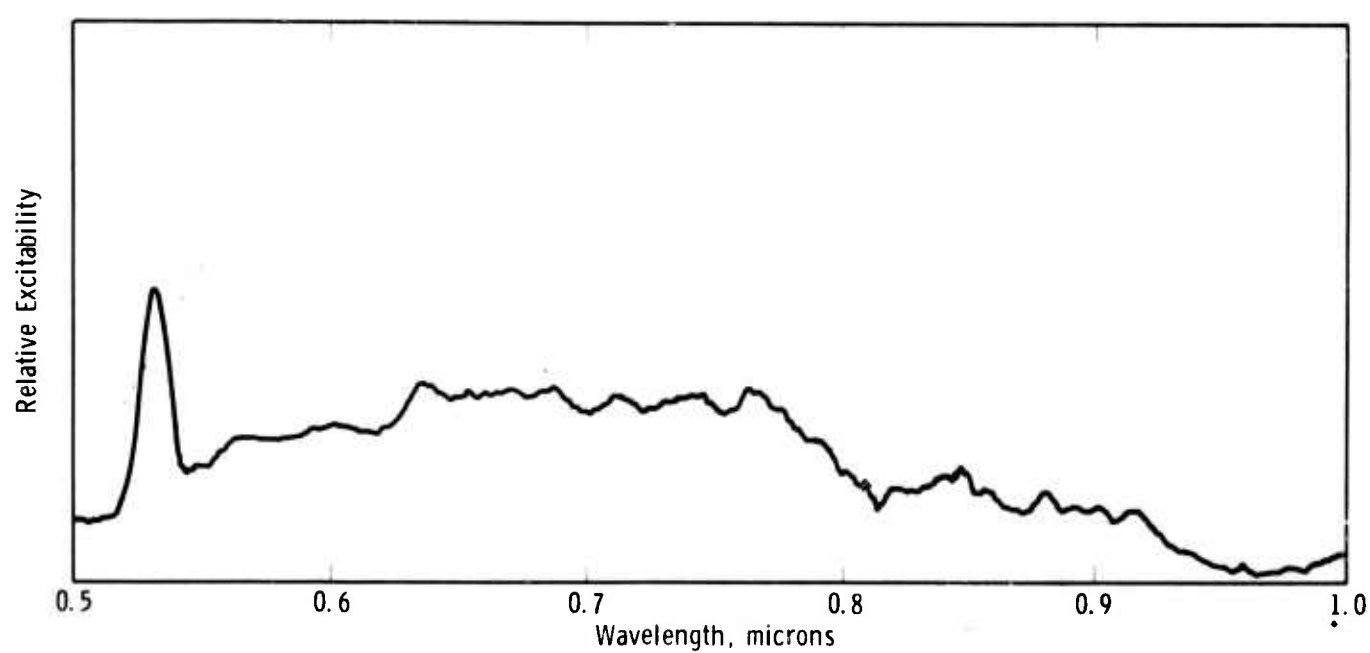


Fig. 18--Excitation spectrum of Ho in YSOAP; $\text{Ho}_{0.2}\text{Cr}_{0.1}$. Compare the broad excitation spectrum of Cr with the spectrum of the rare earth sensitizers shown in Fig. 17.

excitation spectrum of YSOAP:Ho,Cr sample which was prepared before the contract began. The spectrum is included here for reference and for comparison with the spectra of samples with multiple rare-earth sensitization. It is expected that considerably more work will have to be done on this system before it can be realistically evaluated.

3.4 Laser Tests

3.4.1 Apparatus

The apparatus used for testing laser crystals at liquid nitrogen temperature is shown on Fig. 19. The design criteria for the system were: ease of operation, especially with respect to replacement of laser rod; flexibility to handle different sizes of lamps and rods in pulsed and continuous operation; and compatibility with existing equipment such as power supplies, resonator mounts, detectors, Q-switches, etc.

To accomplish this we used:

- 1) a spherical pump light reflector for efficiency,
- 2) external resonators for flexibility,
- 3) flowing liquid nitrogen cooled to below the boiling point for efficient cooling and to avoid gas bubbles around the rod.

The laser rod is mounted inside a double walled pyrex dewar and totally immersed in liquid nitrogen. The liquid nitrogen is cooled to below its boiling point in the overhead reservoir by the cooling device shown at the center of the reservoir. Under the influence of gravity the nitrogen circulates down through the inlet tube, over the laser rod and up to the

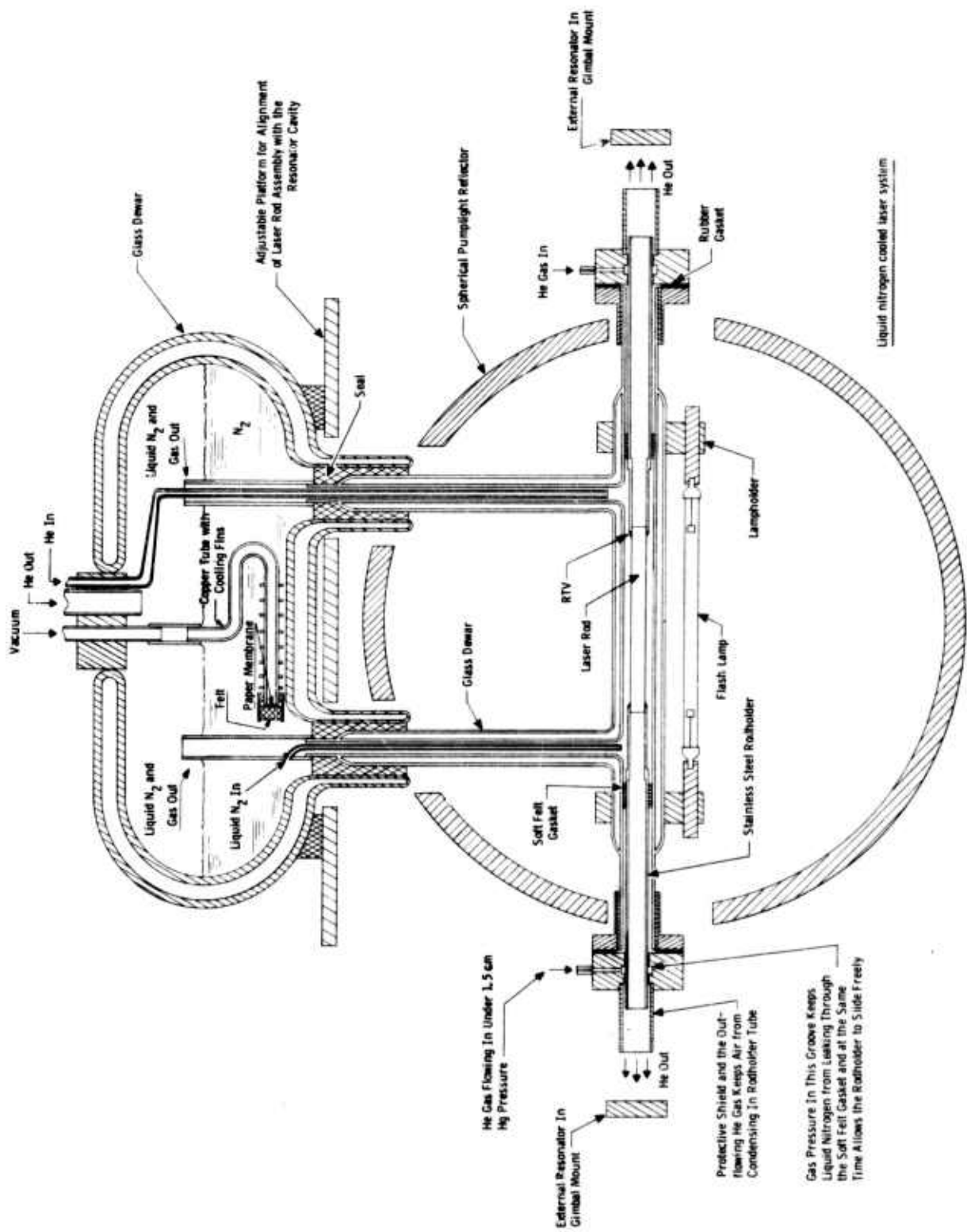


Fig. 19--Liquid nitrogen cooled laser system.

reservoir through the outlet tube. This procedure eliminates air bubbles around the laser rod which would defocus the pumplight.

The laser rod is held in position inside the pyrex jacket by two stainless steel rod holders each of which slides freely in bearings at both ends of the pyrex jacket. The mobility of the holders reduces the stresses introduced in the laser rod resulting from temperature gradients in the system and from the different expansion coefficients of the components. The use of these rod holders makes it possible to employ external resonators, polarizers and Q-switches, thus allowing many experiments to be carried out simply and with little additional fabrication. A silver-coated spherical pump reflector is used to efficiently couple the pump light from the lamp to the laser rod.

3.4.2 Laser Measurements

The system was tested using a 3 mm in. diameter by 30 mm long Er,Tm sensitized, Ho-doped YAG rod (grown by Union Carbide in 1966). This rod had spherical resonators applied directly to the ends; one end was 0.4% transmitting and the other end 99.9% reflecting. When this rod was tested in the system without liquid nitrogen, the room temperature threshold was 98 joules into a Xe 1-1.5 flashlamp. Cooling the rod with liquid nitrogen decreased the threshold to less than 0.6 joules. This was the lowest energy at which the lamp could be fired. The same rod was pumped CW using a small tungsten filament lamp. The threshold was 5 W, and a 12 mW output was obtained with 12 W input to the lamp.

So far only one sensitized YSOAP grown rod has been available for testing. The rod is 25 mm long by 3 mm in diameter and has the

}

composition $\text{CaY}_{2.9}\text{Er}_{0.9}\text{Ho}_{0.1}\text{Tm}_{0.1}(\text{SiO}_4)_3$. It was antireflection coated on both ends and operated with external resonators having 1 meter radius of curvature. The back resonator had 99.9% reflectivity and the output resonators used had reflectivities of 99.9%, 95%, 75% and 55%.

Figure 20 shows the measured threshold energy as a function of output resonator reflectivity. Reference 1 describes how these data may be used to determine the losses in the laser rod. From Fig. 18 we determine a double pass loss of 0.54, corresponding to a loss of about $10\% \text{ cm}^{-1}$. The slope efficiency with 75% output reflectivity was about 0.1%.

We tested some FAP:Ho,Cr rods grown prior to the start of the contract. When external resonators of 99.9% reflectivity were used, one of these rods lased with 28 joules input to the lamp. We noticed several unusual effects while testing this rod. The output of the rod occurred at the very end of the pump pulse even when the rod was pumped with energies of more than 60 joules, i.e., at more than two times threshold. The energy and shape of the output pulse remained the same, independent of input energy when the rod was pumped above threshold. We also noticed a constant increase in threshold throughout the test. Unfortunately no ultraviolet filter were used in the tests and the rod was exposed to flashlamp radiation of wavelength between 0.28μ and 0.4μ . In precontract tests similar laser rods were protected from radiation in that wavelength range and the characteristics mentioned above were not noticed. This leads us to believe that color center formation could be the cause of the problem.

Curve 592843-A

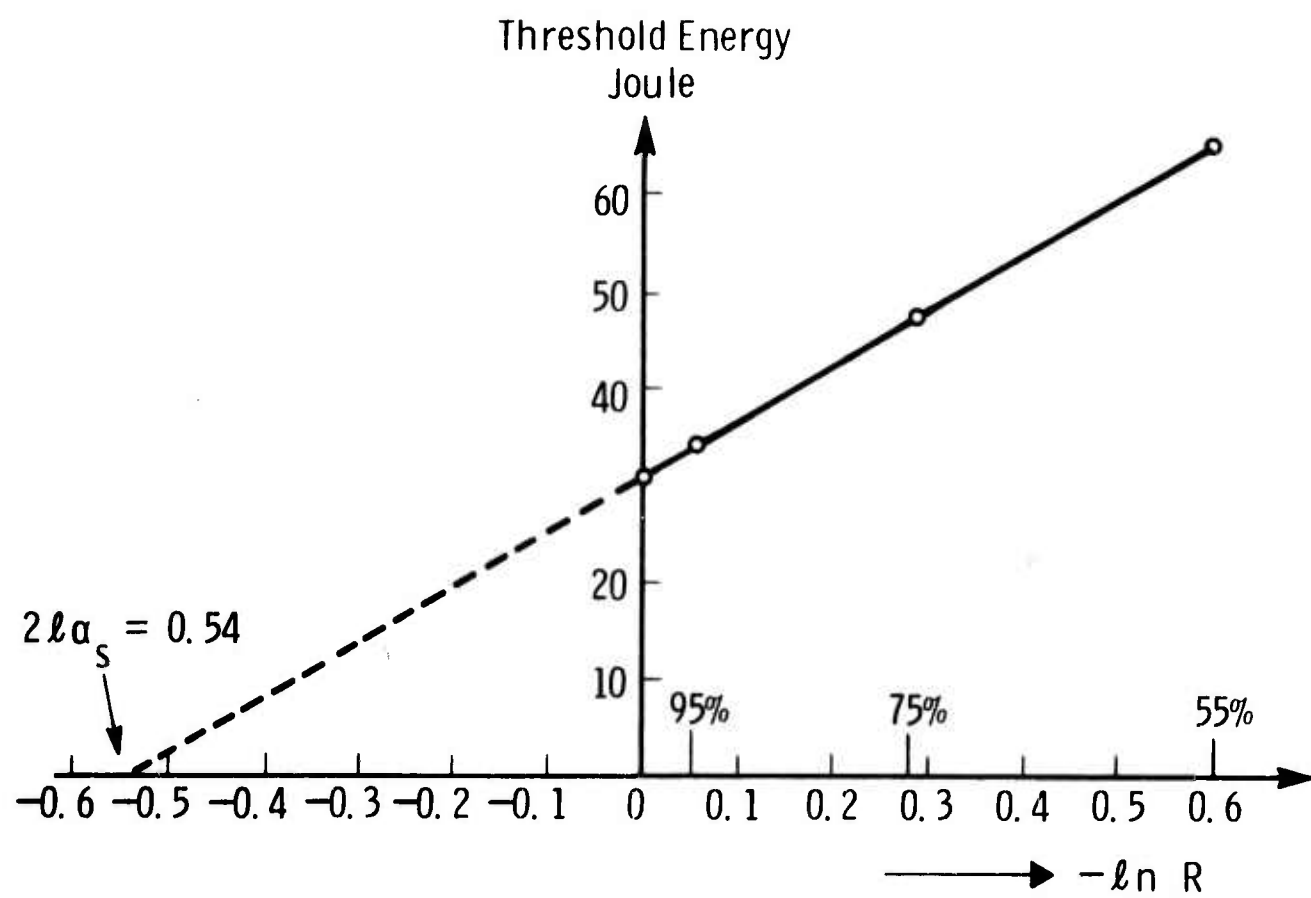


Fig. 20--Threshold energy as a function of output resonator reflectivity
YSOAP 18-203380, 3 mm Dia by 25 mm long, AR coated.

4. DISCUSSION

4.1 Conclusions

Our conclusions regarding this first six-month effort can be summarized as follows: we have adhered closely to the original outline of the effort, and exceeded it in some respects. 1. We have determined what we consider to be the best host material, YSOAP, and essentially completed optimization of the rare-earth sensitizer and activator content for this host. Subject to the qualifications noted in the text, the best laser composition has the formula $\text{CaY}_{2.27}\text{Er}_{1.5}\text{Tm}_{.13}\text{Ho}_{.1}(\text{SiO}_4)_3\text{O}$. 2. We have successfully grown several single crystals of compositions close to the optimum composition, and made some important progress in improving the quality of these crystals. 3. We designed, constructed, and tested an efficient liquid nitrogen laser test assembly which permits quick interchange of samples, allows the laser rod to be completely immersed in liquid nitrogen, if desired, and permits the use of external resonators at both ends of the laser rod. 4. Finally, we have successfully achieved 2.0 micron laser action from the first laser rod grown and tested under this program. The comparatively low threshold (30 joules) of this rod, even considering its very poor optical quality, confirms our expectations of laser performance based upon the results of spectroscopic measurements on polycrystalline samples.

4.2 Future Plans

With the initial phase of determining the best host complete, and with the successful operation of a laser rod, the emphasis of the work will shift towards more crystal development work and laser measurements, and less of the kind of measurements involved in optimization. In the area of crystal preparation, the emphasis will be on growing better laser quality crystals of the YSOAP composition, in particular, growing crystals free of scattering inclusions. In addition crystal growth studies of FAP:Ho,Cr will be resumed. The crystals which are grown will be, for the most part, of compositions suitable for lasers. We expect, therefore, a shift towards more laser tests, and laser evaluation both in pulsed and CW operation. We will begin measurements of the physical properties of SOAP.

Spectroscopic measurements will be continued, but here, too, the emphasis will change towards more detailed measurements, and toward measurements related to laser efficiency. In particular, we intend to perform excitation spectra for most of the material in our possession, and measure lifetimes, and transfer times for sensitizers. We expect to prepare for laser spectroscopy in order to determine the laser wavelengths and laser linewidths. The information obtained from laser tests and spectroscopic measurements will, in turn, be used to improve the laser characteristics, to make adjustments in laser composition, if necessary, and to provide better characterization of the laser materials.

REFERENCES

1. R.C. Ohlmann, K.B. Steinbruegge, and R. Mazelsky, Appl. Optics, V. 7, p. 905 (1968).
2. N.T. Melamed, R. Mazelsky, R.H. Hopkins, et al., Study of Efficiency Improvement of Optically Pumped $\text{Ca}_5(\text{PO}_4)_3\text{F:Nd}$ and $\text{Ca}_5(\text{PO}_4)_3\text{F:Ho,Cr}$, Technical Report AFML-TR-69-184, Air Force Materials Laboratory (1969).
3. A.G. Cockbain and G.V. Smith, Min. Magazine, V. 36, p. 411 (1968).
4. J. Ito, Am. Mineralogist, V. 53, p. 890 (1968).
5. R. Mazelsky, R.H. Hopkins and W.E. Kramer, J. Crystal Growth, V. 3,4, p. 260 (1968).
6. R.H. Hopkins, K.B. Steinbruegge and N.T. Melamed, CW and Q-Switched Capabilities of Nd-doped Calcium Fluorophosphate, Technical Report AFAL-TR-69-239, Air Force Avionics Laboratory (1969).
7. G.M. McManus, R.H. Hopkins and W.J. Takei, J. Appl. Phys., V. 40, p. 180 (1969).
8. B. Cockayne, J. Crystal Growth, V. 3,4, p. 60 (1968).
9. R.H. Hopkins, J. Crystal Growth, V. 6, p. 91 (1969).
10. B. Cockayne and M.P. Gates, J. Mat. Sci., V. 2, p. 118 (1967).
11. D.L. Dexter, J. Chemical Physics, V. 21, p. 836 (1953).

REFERENCES (cont'd)

12. L.F. Johnson, L.G. VanUitert, J.J. Rubin and R.A. Thomas, Phys. Rev., V. 133, p. A494 (1964); L.F. Johnson, J.E. Geusic and L.G. VanUitert, Applied Physics Lett., V 8, p. 200 (1966); R.L. Remski, L.T. James, Jr. K.H. Gooen, B.D. Bartolo, and A. Linz, IEEE J. of Quantum Elect., V. QE-5, p. 214 (1969); R. Hoskins and B.H. Soffer, ibid V. QE-2, p. 253 (1966).
13. E. Snitzer and R. Woodcock, Applied Physics Lett., V. 6, p. 45 (1965).

Security Classification

DOCUMENT CONTROL DATA - R&D

(Security classification of title, body of abstract and indexing annotation must be entered when the overall report is classified)

| | | |
|---|--|--|
| 1. ORIGINATING ACTIVITY (Corporate author) Westinghouse Electric Corporation Research & Development Center | | 2a. REPORT SECURITY CLASSIFICATION UNCLASSIFIED |
| 2b. GROUP | | |
| 3. REPORT TITLE RARE-EARTH DOPED APATITE LASER MATERIALS | | |
| 4. DESCRIPTIVE NOTES (Type of report and inclusive dates) Semi-annual report 19 September 1969 - 19 March 1970 | | |
| 5. AUTHOR(S) (Last name, first name, initial) Hopkins, R.H., Melamed, N.T., Henningsen, T., et al | | |
| 6. REPORT DATE May 1970 | | 7a. TOTAL NO. OF PAGES 65 |
| 8a. CONTRACT OR GRANT NO. <i>C</i> F33615-70-1051 <i>Mel</i> | | 7b. NO. OF REFS 13 |
| 8b. PROJECT NO. ARPA Order 1467 | | 9a. ORIGINATOR'S REPORT NUMBER(S) 70-6J8-REDAP-R1 |
| c. | | 9b. OTHER REPORT NO(S) (Any other numbers that may be assigned this report) AFAL-TR-70-103 |
| 10. AVAILABILITY/LIMITATION NOTICES | | |
| 11. SUPPLEMENTARY NOTES | | 12. SPONSORING MILITARY ACTIVITY Advanced Research Projects Agency Air Force Avionics Laboratory |
| 13. ABSTRACT This first semi-annual report describes the results of the first phase of a program to evaluate the merits of certain members of the mineral family apatite as hosts for the active laser ion holmium. Of the several silicate oxyapatites (SOAP) studied, preliminary crystal growth and spectroscopic measurements indicated that YSOAP, CaY ₄ (SiO ₄) ₃ O, was the most promising laser host. An initial sensitized host composition, believed near optimum for laser action, was derived from spectroscopic measurements on polycrystalline melt samples. This composition, CaY _{2.27} Er _{1.5} Tm _{1.13} Ho _{0.1} (SiO ₄) ₃ O forms the starting point for growth of laser quality crystals. A low temperature, liquid nitrogen-cooled laser testing has been designed and built which is suitable for long pulse, CW, and Q-switched laser operation. The first YSOAP rod grown and tested in this system lased at 77°K with a threshold of 30 joules. | | |

Security Classification

14.

KEY WORDS

| | LINK A | | LINK B | | LINK C | |
|--|--------|----|--------|----|--------|----|
| | ROLE | WT | ROLE | WT | ROLE | WT |
| Lasers Apatite Rare-earth Holmium Erbium Thulium Infrared Crystals Solid-state Ions Doping | | | | | | |

INSTRUCTIONS

1. ORIGINATING ACTIVITY: Enter the name and address of the contractor, subcontractor, grantees, Department of Defense activity or other organization (corporate author) issuing the report.

2a. REPORT SECURITY CLASSIFICATION: Enter the overall security classification of the report. Indicate whether "Restricted Data" is included. Marking is to be in accordance with appropriate security regulations.

2b. GROUP: Automatic downgrading is specified in DoD Directive 5200.10 and Armed Forces Industrial Manual. Enter the group number. Also, when applicable, show that optional markings have been used for Group 3 and Group 4 as authorized.

3. REPORT TITLE: Enter the complete report title in all capital letters. Titles in all cases should be unclassified. If a meaningful title cannot be selected without classification, show title classification in all capitals in parenthesis immediately following the title.

4. DESCRIPTIVE NOTES: If appropriate, enter the type of report, e.g., interim, progress, summary, annual, or final. Give the inclusive dates when a specific reporting period is covered.

5. AUTHOR(S): Enter the name(s) of author(s) as shown on or in the report. Enter last name, first name, middle initial. If military, show rank and branch of service. The name of the principal author is an absolute minimum requirement.

6. REPORT DATE: Enter the date of the report as day, month, year; or month, year. If more than one date appears on the report, use date of publication.

7a. TOTAL NUMBER OF PAGES: The total page count should follow normal pagination procedures, i.e., enter the number of pages containing information.

7b. NUMBER OF REFERENCES: Enter the total number of references cited in the report.

8a. CONTRACT OR GRANT NUMBER: If appropriate, enter the applicable number of the contract or grant under which the report was written.

8b, 8c, & 8d. PROJECT NUMBER: Enter the appropriate military department identification, such as project number, subproject number, system numbers, task number, etc.

9a. ORIGINATOR'S REPORT NUMBER(S): Enter the official report number by which the document will be identified and controlled by the originating activity. This number must be unique to this report.

9b. OTHER REPORT NUMBER(S): If the report has been assigned any other report numbers (either by the originator or by the sponsor), also enter this number(s).

10. AVAILABILITY/LIMITATION NOTICES: Enter any limitations on further dissemination of the report, other than those

imposed by security classification, using standard statements such as:

- (1) "Qualified requesters may obtain copies of this report from DDC."
- (2) "Foreign announcement and dissemination of this report by DDC is not authorized."
- (3) "U. S. Government agencies may obtain copies of this report directly from DDC. Other qualified DDC users shall request through . . ."
- (4) "U. S. military agencies may obtain copies of this report directly from DDC. Other qualified users shall request through . . ."
- (5) "All distribution of this report is controlled. Qualified DDC users shall request through . . ."

If the report has been furnished to the Office of Technical Services, Department of Commerce, for sale to the public, indicate this fact and enter the price, if known.

11. SUPPLEMENTARY NOTES: Use for additional explanatory notes.

12. SPONSORING MILITARY ACTIVITY: Enter the name of the departmental project office or laboratory sponsoring (paying for) the research and development. Include address.

13. ABSTRACT: Enter an abstract giving a brief and factual summary of the document indicative of the report, even though it may also appear elsewhere in the body of the technical report. If additional space is required, a continuation sheet shall be attached.

It is highly desirable that the abstract of classified reports be unclassified. Each paragraph of the abstract shall end with an indication of the military security classification of the information in the paragraph, represented as (TS), (S), (C), or (U).

There is no limitation on the length of the abstract. However, the suggested length is from 150 to 225 words.

14. KEY WORDS: Key words are technically meaningful terms or short phrases that characterize a report and may be used as index entries for cataloging the report. Key words must be selected so that no security classification is required. Identifiers, such as equipment model designation, trade name, military project code name, geographic location, may be used as key words but will be followed by an indication of technical context. The assignment of links, rules, and weights is optional.